Computers and Mathematics with Applications 117 (2022) 312–325

Contents lists available at ScienceDirect

Computers and Mathematics with Applications

www.elsevier.com/locate/camwa

Goal-oriented a posteriori error estimation for the biharmonic problem based on an equilibrated moment tensor

Gouranga Mallik

Department of Mathematics, Indian Institute of Science, Bangalore 560012, India

ARTICLE INFO

Keywords:
Quantity of interest
A posteriori error estimate
Guaranteed bound
Equilibrated moment tensor
Unified framework
Adaptivity

ABSTRACT

In this article, we discuss goal-oriented a posteriori error estimation for the biharmonic plate bending problem. The error for a numerical approximation of a goal functional is represented by several computable estimators. One of these estimators is obtained using the dual-weighted residual method, which takes advantage of an equilibrated moment tensor. Then, an abstract unified framework for the goal-oriented a posteriori error estimation is derived based on the equilibrated moment tensor and the potential reconstruction that provides a guaranteed upper bound for the error of a numerical approximation for the goal functional. In particular, C^0 interior penalty and discontinuous Galerkin finite element methods are employed for the practical realisation of the estimators. Numerical experiments are performed to illustrate the effectivity of the estimators.

1. Introduction

Adjoint-based goal-oriented a posteriori error estimation is an efficient tool for the numerical approximation of many engineering problems as it provides relevant information about the error in a quantity of interest rather than the error estimation derived in some norm or seminorm. Goal-oriented a posteriori error estimation was initially proposed by Becker and Rannacher [3] and Prudhomme and Oden [34,32] using the dual-weighted residual (DWR) method (see [21,2,11,30] for subsequent works). Some of the popular approaches on the goal-oriented a posteriori error estimation are the multi-objective goal functional error estimation of [39,17,25], the constitutive relation error (CRE) of [26,28,37,35,36], the enhanced least-squares finite element methods of [13], the combination of DWR, and the equilibrated flux of [31], the guaranteed bounds based on the equilibrated flux of [29,1].

Traditionally, an a posteriori error analysis hinges upon the computation of the residual [2]

$$a(u-u_h,v)=l(v)-a(u_h,v)=:\rho(u_h)(v)$$

for some bilinear form $a(\bullet,\bullet)$ and linear form l associated with elliptic partial differential equations (PDEs) with u and u_h being its weak and Galerkin solutions, and v being a test function. By incorporating a goal-functional Q in a dual problem $a(v,z)=Q(v)$ for all test functions v, and using Galerkin orthogonality, we have

$$Q(u-u_h)=a(u-u_h,z)=a(u-u_h,z-v_h)=\rho(u_h)(z-v_h)$$

for all discrete functions v_h. This approach involves the computation of an estimator weighted with the solution related to the dual problem. For the computational purpose, a suitable residual-based estimator can be chosen for the primal problem, and the dual-problem solution z can be replaced by a discrete solution obtained in some finer discretization space. However, in most cases, the estimators involve unknown constants; hence they do not provide a guaranteed a posteriori error bound. In order to obtain a guaranteed a posteriori estimator, one often incorporates the equilibrated flux (see [29,28]). Much research has been conducted regarding the goal-oriented a posteriori estimation for second-order PDEs. However, to the author's knowledge, there are very few results (except [22]) on the goal-oriented a posteriori error estimation for fourth-order PDEs. An *hp*-discontinuous Galerkin DWR-based goal error estimation has been proposed by [22] for the biharmonic problem and applied to describe the displacement of a thin and isotropic homogeneous plate and the stream function formulation of the Stokes fluid problem that describes the flow of a viscous fluid around a flat plate.

The article's main purpose is to develop a unified framework for goal-oriented a posteriori error estimation for a model linear biharmonic problem. We consider goal functional of the form $Q(u)=(\tilde{f},u)$ for a weight function $\tilde{f}\in L^2(\Omega)$. In practical applications, this can be applied to approximate the goal functional governed by mean deflection around a specified zone and point deflection at some point (in a regularized form). This framework is applied (but not limited) to C^0 interior penalty and discontinuous Galerkin finite element methods. We

E-mail address: gourangam@iisc.ac.in.

https://doi.org/10.1016/j.camwa.2022.04.021
Received 14 July 2021; Received in revised form 19 April 2022; Accepted 27 April 2022
Available online 20 May 2022

also establish a goal estimator that combines the DWR approach and the equilibrated moment tensor for the primal and dual problems. Finally, a unified guaranteed a posteriori error estimation is established through the potential reconstruction and the equilibrated moment tensor, which is significantly different from the DWR method of [22].

The organization of the paper is as follows. In Section 2, we define some notations and present some preliminary results. In Section 3, we introduce a model problem and state some useful results. In Section 4, we establish some a posteriori error estimates for the goal functional. In Section 5, we consider finite element discretization for the approximation of solution and address some applications of the abstract framework. Finally, in Section 6, we perform some numerical tests to substantiate the theoretical results.

2. Setting

Let $\Omega \subset \mathbb{R}^2$ be a bounded polygonal domain with the boundary $\partial\Omega$. Throughout the paper, standard notations on Lebesgue and Sobolev spaces and their norms are employed. We denote the L^2 scalar or vector inner product by $(\bullet,\bullet)$. The standard semi-norm and norm on $H^s(\Omega)$ (resp. $W^{s,p}(\Omega)$) for $s>0$ are denoted by $|\bullet|_s$ and $\|\bullet\|_s$ (resp. $|\bullet|_{s,p}$ and $\|\bullet\|_{s,p}$). We refer $H^{-m}(\Omega)$ to be the dual space of $H_0^m(\Omega)$ with $\langle\bullet,\bullet\rangle_m$ denoting the duality product and for $m=2$ we often denote the duality product simply by $\langle\bullet,\bullet\rangle$. Further, let $\boldsymbol{H}(\mathrm{div},\Omega)$ be the Hilbert space of vector fields $\underline{q} \in [L^2(\Omega)]^2$ such that $\nabla\cdot\underline{q} \in L^2(\Omega)$. Any matrix valued function in $[L^2(\Omega)]^{2\times 2}$ is denoted by $\underline{\underline{q}} = (q_{ij})_{i,j=1}^2$ and the inner-product reads $(\underline{\underline{p}},\underline{\underline{q}}) = \int_\Omega \underline{\underline{p}} : \underline{\underline{q}}\,\mathrm{dx}$, where $\underline{\underline{p}} : \underline{\underline{q}} = \sum_{i,j=1}^2 p_{ij}q_{ij}$. Moreover, we introduce the Hilbert space

$$\underline{\underline{\boldsymbol{H}}} := \left\{ \underline{\underline{q}} \in \boldsymbol{H}(\mathrm{div},\Omega)^2 : \nabla\cdot\underline{\underline{q}} \in \boldsymbol{H}(\mathrm{div},\Omega) \right\}.$$

Finally, we refer to $D^2v := (\partial^2 v/\partial x_i\partial x_j)_{i,j=1}^2$ as the matrix of second order partial derivatives of a function $v \in H^2(\Omega)$. The set of all symmetric 2×2 matrix valued functions is denoted by $[L^2(\Omega)]^{2\times 2}_{\mathrm{sym}}$.

Let $\mathcal{T}_h$ be a shape-regular [4] triangulation of Ω into closed triangles. The set of all internal vertices (resp. boundary vertices) and interior edges (resp. boundary edges) of the triangulation $\mathcal{T}_h$ are denoted by $\mathcal{N}_h(\Omega)$ (resp. $\mathcal{N}_h(\partial\Omega)$) and $\mathcal{E}_h(\Omega)$ (resp. $\mathcal{E}_h(\partial\Omega)$). Define a piecewise constant mesh function $h_{\mathcal{T}_h}(x) = h_K = \mathrm{diam}(K)$ for all $x \in K$, $K \in \mathcal{T}_h$, and set $h := \max_{K\in\mathcal{T}_h} h_K$. Also define a piecewise constant edge-function on $\mathcal{E}_h := \mathcal{E}_h(\Omega)\cup\mathcal{E}_h(\partial\Omega)$ by $h_{\mathcal{E}_h}|_e = h_e = \mathrm{diam}(e)$ for any $e \in \mathcal{E}_h$. The set of all edges of K is denoted by $\mathcal{E}_h(K)$. Note that for a shape-regular family, there exists a positive constant C independent of h such that any $K \in \mathcal{T}_h$ and any $e \in \mathcal{E}_h(K)$ satisfy $Ch_K \le h_e \le h_K$. Let $\mathbb{P}_k(K)$ denote the set of all polynomials of degree less than or equal to k and

$$\mathbb{P}_k(\mathcal{T}_h) := \left\{ \varphi \in L^2(\Omega) : \forall K \in \mathcal{T}_h, \varphi|_K \in \mathbb{P}_k(K) \right\}.$$

The $L^2(\Omega)$ projection onto $\mathbb{P}_k(\mathcal{T}_h)$ is denoted by Π_k. For a non-negative integer s, define the broken Sobolev space for the subdivision $\mathcal{T}_h$ as

$$H^s(\mathcal{T}_h) = \left\{ \varphi \in L^2(\Omega) : \varphi|_K \in H^s(K) \quad \forall K \in \mathcal{T}_h \right\},$$

with the broken Sobolev semi-norm $|\bullet|_{H^s(\mathcal{T}_h)}$ and norm $\|\bullet\|_{H^s(\mathcal{T}_h)}$ defined by

$$|\varphi|_{H^s(\mathcal{T}_h)} = \left(\sum_{K\in\mathcal{T}_h} |\varphi|^2_{H^s(K)} \right)^{1/2} \text{ and } \|\varphi\|_{H^s(\mathcal{T}_h)} = \left(\sum_{K\in\mathcal{T}_h} \|\varphi\|^2_{H^s(K)} \right)^{1/2}.$$

Define the jump $[\![\varphi]\!]_e = \varphi|_{K_+} - \varphi|_{K_-}$ and the average $\{\!\{\varphi\}\!\}_e = \frac{1}{2}\left(\varphi|_{K_+} + \varphi|_{K_-}\right)$ across the interior edge e of $\varphi \in H^1(\mathcal{T}_h)$ of the adjacent triangles K_+ and K_-. Extend the definition of the jump and the average to an edge lying on the boundary by $[\![\varphi]\!]_e = \varphi|_e$ and $\{\!\{\varphi\}\!\}_e = \varphi|_e$ when e belongs to the set of boundary edges $\mathcal{E}_h(\partial\Omega)$. For any vector function, the jump and the average are understood componentwise.

There exist real numbers C_{tr} and $C_{\mathrm{tr,c}}$ independent of h such that the following discrete and continuous trace inequalities hold for all $K \in \mathcal{T}_h$ and $e \in \mathcal{E}_h$ (see [16, Lemma 1.46 and 1.49])

$$\|v\|_e \le C_{\mathrm{tr}} h_e^{-1/2} \|v\|_K \quad \forall v \in \mathbb{P}_k(K),$$
$$\|v\|_{\partial K} \le C_{\mathrm{tr,c}} (h_K^{-1}\|v\|_T^2 + h_K\|\nabla v\|_K^2)^{1/2} \quad \forall v \in H^1(K).$$

The positive constants C appearing in the inequalities denote generic constants that do not depend on mesh-size. The notation $a \lesssim b$ means that there exists a generic constant C independent of the mesh parameters such that $a \le Cb$.

3. Model problem

In this article, we are interested in the goal-oriented a posteriori error estimations for a general linear fourth-order boundary-value problem, but the results can be extended to more general situations. For simplicity of presentation, we restrict ourselves to a simple model problem. Consider the biharmonic equation with the clamped boundary conditions

$$\Delta^2 u = f \quad \text{in } \Omega, \tag{3.1a}$$
$$u = 0 = \frac{\partial u}{\partial \nu} \quad \text{on } \partial\Omega, \tag{3.1b}$$

where $\Delta^2 u = \Delta(\Delta u)$ and the source term f. Define $V := H_0^2(\Omega)$. The weak formulation of (3.1) is given by: for $f \in H^{-2}(\Omega)$, find $u \in V$ such that

$$(D^2u, D^2v) = \langle f, v\rangle \quad \forall\, v \in V. \tag{3.2}$$

In this article, we are interested in the following goal functional

$$Q(u) = (\tilde{f}, u) \tag{3.3}$$

for a chosen weight function $\tilde{f} \in L^2(\Omega)$. We analyse the above goal functional by a dual problem of (3.1) that consists of finding $\tilde{u} : \Omega \to \mathbb{R}$ such that

$$\Delta^2 \tilde{u} = \tilde{f} \quad \text{in } \Omega, \tag{3.4a}$$
$$\tilde{u} = 0 = \frac{\partial \tilde{u}}{\partial \nu} \quad \text{on } \partial\Omega. \tag{3.4b}$$

The weak formulation seeks $\tilde{u} \in V$ such that

$$(D^2\tilde{u}, D^2v) = (\tilde{f}, v) \quad \forall\, v \in V. \tag{3.5}$$

The existence and uniqueness of the weak solution of the primal and the dual problems (3.2) and (3.5) follow from the Riesz representation theorem.

We state two definitions that are essential for establishing some a posteriori error estimations for the numerical approximation of the goal functional Q of (3.3).

Definition 3.1 *(Potential reconstruction).* Any function s_h (resp. $\tilde{s}_h$) constructed from u_h (resp. $\tilde{u}_h$) which satisfies

$$s_h \in H_0^2(\Omega)\cap C^1(\bar{\Omega}) \quad (\text{resp. } \tilde{s}_h \in H_0^2(\Omega)\cap C^1(\bar{\Omega})) \tag{3.6}$$

is called a potential reconstruction.

Throughout the article, we understand the $\mathrm{div}\,\mathrm{div}$ operator in the distributional sense, i.e., for $\underline{\underline{\tau}} \in [L^2(\Omega)]^{2\times 2}_{\mathrm{sym}}$

$$\langle \mathrm{div}\,\mathrm{div}\,\underline{\underline{\tau}}, w\rangle = \int_\Omega \underline{\underline{\tau}} : D^2 w\,\mathrm{dx}, \qquad \forall\, w \in H_0^2(\Omega).$$

Definition 3.2 *(Equilibrated moment tensor).* Let $f_h \in H^{-2}(\Omega)$ (resp. $\tilde{f}_h \in H^{-2}(\Omega)$). Any matrix valued function $\underline{\underline{\boldsymbol{\sigma}}}_h^{\mathrm{eq}} \in [L^2(\Omega)]^{2\times 2}_{\mathrm{sym}}$ (resp. $\underline{\underline{\tilde{\boldsymbol{\sigma}}}}_h^{\mathrm{eq}} \in [L^2(\Omega)]^{2\times 2}_{\mathrm{sym}}$) which satisfies

$$\langle \operatorname{div}\operatorname{div} \underline{\underline{\boldsymbol{\sigma}}}_h^{\mathrm{eq}}, w\rangle = \langle f_h, w\rangle \quad \forall\, w \in H_0^2(\Omega) \tag{3.7a}$$

$$(\text{resp. } \langle \operatorname{div}\operatorname{div} \underline{\underline{\tilde{\boldsymbol{\sigma}}}}_h^{\mathrm{eq}}, w\rangle = \langle \tilde{f}_h, w\rangle \quad \forall\, w \in H_0^2(\Omega)) \tag{3.7b}$$

is called an equilibrated moment tensor.

The construction of the potential reconstruction of Definition 3.1 can be found in [7,14,8,20], and the equilibrated moment tensor of Definition 3.2 can be found in [5,6]. We briefly describe their constructions in Section 5. We state the following Prager–Synge type [33] energy principle and refer to [5, Theorem 3.2] and [6, Theorem 3.1] for the proof.

Lemma 3.3 *(Two-energies principle for the biharmonic equation). Let $f_h \in H^{-2}(\Omega)$ and $\hat{u} \in H_0^2(\Omega)$ be the solution of the biharmonic equation*

$$(D^2\hat{u}, D^2 w) = \langle f_h, w\rangle \quad \forall\, w \in H_0^2(\Omega).$$

For $v \in H_0^2(\Omega)$, the tensor $\underline{\underline{\boldsymbol{\sigma}}}_h^{\mathrm{eq}} \in [L^2(\Omega)]^{2\times 2}_{\mathrm{sym}}$ defined in Definition 3.2 satisfies [33,6]

$$\|D^2(\hat{u}-v)\|^2 + \|D^2\hat{u} - \underline{\underline{\boldsymbol{\sigma}}}_h^{\mathrm{eq}}\|^2 = \|D^2 v - \underline{\underline{\boldsymbol{\sigma}}}_h^{\mathrm{eq}}\|^2.$$

Moreover, let $u \in H_0^2(\Omega)$ (resp. $\tilde{u} \in H_0^2(\Omega)$) be the solution of (3.2) (resp. (3.5)). Then for any $v \in H_0^2(\Omega)$ (resp. $\tilde{v} \in H_0^2(\Omega)$), the following also holds

$$\|D^2(u-v)\|^2 + \|D^2 u - \underline{\underline{\boldsymbol{\sigma}}}_h^{\mathrm{eq}}\|^2 = \|D^2 v - \underline{\underline{\boldsymbol{\sigma}}}_h^{\mathrm{eq}}\|^2 + 2\langle f - f_h, u - v\rangle.$$

$$(\text{resp. } \|D^2(\tilde{u}-\tilde{v})\|^2 + \|D^2\tilde{u} - \underline{\underline{\tilde{\boldsymbol{\sigma}}}}_h^{\mathrm{eq}}\|^2 = \|D^2\tilde{v} - \underline{\underline{\tilde{\boldsymbol{\sigma}}}}_h^{\mathrm{eq}}\|^2 + 2\langle \tilde{f} - \tilde{f}_h, \tilde{u} - \tilde{v}\rangle.) \tag{3.8}$$

4. Goal-oriented error estimates

In this section, we present some approximations for the goal functional. Then the goal error is decomposed into computable estimators. Choosing $v = u$ in (3.5) and $v = \tilde{u}$ in (3.2), the following primal-dual equivalence relation holds

$$Q(u) = (\tilde{f}, u) = (D^2\tilde{u}, D^2 u) = (D^2 u, D^2\tilde{u}) = \langle f, \tilde{u}\rangle. \tag{4.1}$$

The goal functional is approximated in the following subsections, and some error representations are presented.

4.1. Some residual type goal error estimations

In this subsection, the goal error is represented by an estimator and a remainder term. For any edge $e \in \mathcal{E}_h$, the outward unit normal across the edge is denoted by $\boldsymbol{n}_e$ and unit tangent along the edge is denoted by $\boldsymbol{\tau}_e$. Define $\partial_n v := \nabla v \cdot \boldsymbol{n}_e$, $D^2_{nn} v := \boldsymbol{n}_e^T D^2 v \boldsymbol{n}_e$ and $\sigma^{\mathrm{eq}}_{h,nn} := \boldsymbol{n}_e^T \underline{\underline{\boldsymbol{\sigma}}}_h^{\mathrm{eq}} \boldsymbol{n}_e, \sigma^{\mathrm{eq}}_{h,n\tau} := \boldsymbol{\tau}_e^T \underline{\underline{\boldsymbol{\sigma}}}_h^{\mathrm{eq}} \boldsymbol{n}_e$.

Theorem 4.1 *(Error representation of the goal functional). Let u and $\tilde{u} \in H_0^2(\Omega)$ respectively be the solutions of (3.1) and (3.4). Let u_h and $\tilde{u}_h \in \mathbb{P}_k(\mathcal{T}_h)$ respectively be arbitrary piecewise polynomial approximations for u and $\tilde{u}$. Let $\tilde{s}_h$ be the potential reconstructions of Definition 3.1, and $\underline{\underline{\boldsymbol{\sigma}}}_h^{\mathrm{eq}}$ and $\underline{\underline{\tilde{\boldsymbol{\sigma}}}}_h^{\mathrm{eq}}$ be the equilibrated moment tensors of Definition 3.2 constructed from u_h and $\tilde{u}_h$ respectively. Then the goal error is expressed as*

$$Q(u) - Q(u_h) = \eta^{\mathrm{res}}_{h,\mathrm{goal}}(u_h, \tilde{u}_h; \underline{\underline{\boldsymbol{\sigma}}}_h^{\mathrm{eq}}, \underline{\underline{\tilde{\boldsymbol{\sigma}}}}_h^{\mathrm{eq}}) + \mathcal{R}^{\mathrm{res}}_{h,\mathrm{rem}}(u, \tilde{u}, f; u_h, \tilde{u}_h), \tag{4.2}$$

where the estimator is given by

$$\begin{aligned}
\eta^{\mathrm{res}}_{h,\mathrm{goal}}(u_h, \tilde{u}_h; \underline{\underline{\boldsymbol{\sigma}}}_h^{\mathrm{eq}}, \underline{\underline{\tilde{\boldsymbol{\sigma}}}}_h^{\mathrm{eq}}) &:= \langle f, \tilde{s}_h\rangle - \sum_{K\in\mathcal{T}_h}\int_K \underline{\underline{\boldsymbol{\sigma}}}_h^{\mathrm{eq}} : D^2\tilde{s}_h \,\mathrm{dx} \\
&+ \sum_{K\in\mathcal{T}_h}\int_K (\underline{\underline{\boldsymbol{\sigma}}}_h^{\mathrm{eq}} - D^2 u_h) : \underline{\underline{\tilde{\boldsymbol{\sigma}}}}_h^{\mathrm{eq}} \,\mathrm{dx} \\
&+ \sum_{e\in\mathcal{E}_h}\int_e \llbracket \partial_\tau u_h \rrbracket_e \, \tilde{\sigma}^{\mathrm{eq}}_{h,n\tau} \,\mathrm{ds} + \sum_{e\in\mathcal{E}_h}\int_e \llbracket \partial_n u_h \rrbracket_e \, \tilde{\sigma}^{\mathrm{eq}}_{h,nn} \,\mathrm{ds} \\
&+ \sum_{e\in\mathcal{E}_h}\int_e \llbracket u_h \rrbracket_e \operatorname{div} \underline{\underline{\tilde{\boldsymbol{\sigma}}}}_h^{\mathrm{eq}} \cdot \boldsymbol{n}_e \,\mathrm{ds},
\end{aligned} \tag{4.3}$$

with remainder term

$$\begin{aligned}
&\mathcal{R}^{\mathrm{res}}_{h,\mathrm{rem}}(u, \tilde{u}, f; u_h, \tilde{u}_h) : \\
&= \langle f - \operatorname{div}\operatorname{div} \underline{\underline{\boldsymbol{\sigma}}}_h^{\mathrm{eq}}, \tilde{u} - \tilde{s}_h\rangle + \sum_{K\in\mathcal{T}_h}\int_K (\underline{\underline{\boldsymbol{\sigma}}}_h^{\mathrm{eq}} - D^2 u_h) : (D^2\tilde{u} - \underline{\underline{\tilde{\boldsymbol{\sigma}}}}_h^{\mathrm{eq}}) \,\mathrm{dx} \\
&+ \sum_{e\in\mathcal{E}_h}\int_e \llbracket \partial_\tau u_h \rrbracket_e \, (D^2_{n\tau}\tilde{u} - \tilde{\sigma}^{\mathrm{eq}}_{h,n\tau}) \,\mathrm{ds} + \sum_{e\in\mathcal{E}_h}\int_e \llbracket \partial_n u_h \rrbracket_e \, (D^2_{nn}\tilde{u} - \tilde{\sigma}^{\mathrm{eq}}_{h,nn}) \,\mathrm{ds} \\
&+ \sum_{e\in\mathcal{E}_h}\int_e \llbracket u_h \rrbracket_e \, (\operatorname{div}(D^2\tilde{u}) - \operatorname{div} \underline{\underline{\tilde{\boldsymbol{\sigma}}}}_h^{\mathrm{eq}}) \cdot \boldsymbol{n}_e \,\mathrm{ds}.
\end{aligned} \tag{4.4}$$

Proof. The primal-dual equivalence relation (4.1) and the definition of goal functional (3.3) lead to the goal error representation

$$Q(u) - Q(u_h) = \langle f, \tilde{u}\rangle - (\tilde{f}, u_h). \tag{4.5}$$

The second term of the above equation is expressed using the solution of the dual problem (3.4) and successive application of the integration by parts as

$$\begin{aligned}
(\tilde{f}, u_h) &= \sum_{K\in\mathcal{T}_h}\int_K u_h \Delta^2\tilde{u} \,\mathrm{dx} = \sum_{K\in\mathcal{T}_h}\int_K u_h \operatorname{div}\operatorname{div}(D^2\tilde{u}) \,\mathrm{dx} \\
&= -\sum_{K\in\mathcal{T}_h}\int_K \nabla u_h \cdot \operatorname{div}(D^2\tilde{u}) \,\mathrm{dx} + \sum_{K\in\mathcal{T}_h}\int_{\partial K} u_h \operatorname{div}(D^2\tilde{u}) \cdot \boldsymbol{n} \,\mathrm{ds} \\
&= \sum_{K\in\mathcal{T}_h}\int_K D^2 u_h : D^2\tilde{u} \,\mathrm{dx} - \sum_{K\in\mathcal{T}_h}\int_{\partial K} \nabla u_h \cdot D^2\tilde{u}\boldsymbol{n} \,\mathrm{ds} \\
&\quad + \sum_{K\in\mathcal{T}_h}\int_{\partial K} u_h \operatorname{div}(D^2\tilde{u}) \cdot \boldsymbol{n} \,\mathrm{ds}.
\end{aligned}$$

Expressing the gradient in the tangent-normal direction as $\nabla u_h = \partial_\tau u_h \boldsymbol{\tau}_e + \partial_n u_h \boldsymbol{n}_e$ and summing over all the edges, we obtain the following expression for the above equation as

$$\begin{aligned}
(\tilde{f}, u_h) &= \sum_{K\in\mathcal{T}_h}\int_K D^2 u_h : D^2\tilde{u} \,\mathrm{dx} - \sum_{e\in\mathcal{E}_h}\int_e \llbracket \partial_\tau u_h \rrbracket_e \, D_{n\tau}\tilde{u} \,\mathrm{ds} \\
&\quad - \sum_{e\in\mathcal{E}_h}\int_e \llbracket \partial_n u_h \rrbracket_e \, D_{nn}\tilde{u} \,\mathrm{ds} + \sum_{e\in\mathcal{E}_h}\int_e \llbracket u_h \rrbracket_e \operatorname{div}(D^2\tilde{u}) \cdot \boldsymbol{n}_e \,\mathrm{ds}.
\end{aligned} \tag{4.6}$$

The above two displayed equations (4.5) and (4.6) lead to

$$\begin{aligned}
Q(u) - Q(u_h) = \langle f, \tilde{u}\rangle &- \sum_{K\in\mathcal{T}_h}\int_K D^2 u_h : D^2\tilde{u} \,\mathrm{dx} + \sum_{e\in\mathcal{E}_h}\int_e \llbracket \partial_\tau u_h \rrbracket_e \, D_{n\tau}\tilde{u} \,\mathrm{ds} \\
&+ \sum_{e\in\mathcal{E}_h}\int_e \llbracket \partial_n u_h \rrbracket_e \, D_{nn}\tilde{u} \,\mathrm{ds} \\
&- \sum_{e\in\mathcal{E}_h}\int_e \llbracket u_h \rrbracket_e \operatorname{div}(D^2\tilde{u}) \cdot \boldsymbol{n}_e \,\mathrm{ds}.
\end{aligned} \tag{4.7}$$

Introducing the equilibrated moment tensor $\underline{\underline{\boldsymbol{\sigma}}}_h^{\mathrm{eq}}$ and $\underline{\underline{\tilde{\boldsymbol{\sigma}}}}_h^{\mathrm{eq}}$ of Definition 3.2 in the first two terms of the above equation (4.7) yields

$$\begin{aligned}
&\langle f,\tilde{u}\rangle - \sum_{K\in\mathcal{T}_h}\int_K D^2u_h : D^2\tilde{u}\,\mathrm{d}x\\
&= \langle f - \operatorname{div}\operatorname{div}\underline{\underline{\boldsymbol{\sigma}}}_h^{\mathrm{eq}},\tilde{u}\rangle + \int_\Omega \underline{\underline{\boldsymbol{\sigma}}}_h^{\mathrm{eq}} : D^2\tilde{u}\,\mathrm{d}x - \sum_{K\in\mathcal{T}_h}\int_K D^2u_h : D^2\tilde{u}\,\mathrm{d}x\\
&= \langle f - \operatorname{div}\operatorname{div}\underline{\underline{\boldsymbol{\sigma}}}_h^{\mathrm{eq}},\tilde{s}_h\rangle + \langle f - \operatorname{div}\operatorname{div}\underline{\underline{\boldsymbol{\sigma}}}_h^{\mathrm{eq}},\tilde{u}-\tilde{s}_h\rangle\\
&\quad + \sum_{K\in\mathcal{T}_h}\int_K (\underline{\underline{\boldsymbol{\sigma}}}_h^{\mathrm{eq}} - D^2u_h) : \underline{\underline{\tilde{\boldsymbol{\sigma}}}}_h^{\mathrm{eq}}\,\mathrm{d}x + \sum_{K\in\mathcal{T}_h}\int_K (\underline{\underline{\boldsymbol{\sigma}}}_h^{\mathrm{eq}} - D^2u_h) : (D^2\tilde{u} - \underline{\underline{\tilde{\boldsymbol{\sigma}}}}_h^{\mathrm{eq}})\,\mathrm{d}x.
\end{aligned} \tag{4.8}$$

The first two terms in the above equation can be written as

$$\begin{aligned}
&\langle f - \operatorname{div}\operatorname{div}\underline{\underline{\boldsymbol{\sigma}}}_h^{\mathrm{eq}},\tilde{s}_h\rangle + \langle f - \operatorname{div}\operatorname{div}\underline{\underline{\boldsymbol{\sigma}}}_h^{\mathrm{eq}},\tilde{u}-\tilde{s}_h\rangle\\
&\quad = \langle f,\tilde{s}_h\rangle - (\underline{\underline{\boldsymbol{\sigma}}}_h^{\mathrm{eq}}, D^2\tilde{s}_h) + \langle f - f_h,\tilde{u}-\tilde{s}_h\rangle.
\end{aligned} \tag{4.9}$$

Introducing the equilibrated moment tensor of tangent-normal directions in the third and fourth terms of (4.7), we obtain

$$\begin{aligned}
&\sum_{e\in\mathcal{E}_h}\int_e \llbracket\partial_\tau u_h\rrbracket_e\, D_{n\tau}\tilde{u}\,\mathrm{d}s + \sum_{e\in\mathcal{E}_h}\int_e \llbracket\partial_n u_h\rrbracket_e\, D_{nn}\tilde{u}\,\mathrm{d}s\\
&= \sum_{e\in\mathcal{E}_h}\int_e \llbracket\partial_\tau u_h\rrbracket_e\, \tilde{\sigma}^{\mathrm{eq}}_{h,n\tau}\,\mathrm{d}s + \sum_{e\in\mathcal{E}_h}\int_e \llbracket\partial_n u_h\rrbracket_e\, \tilde{\sigma}^{\mathrm{eq}}_{h,nn}\,\mathrm{d}s\\
&\quad + \sum_{e\in\mathcal{E}_h}\int_e \llbracket\partial_\tau u_h\rrbracket_e\, (D_{n\tau}\tilde{u} - \tilde{\sigma}^{\mathrm{eq}}_{h,n\tau})\,\mathrm{d}s + \sum_{e\in\mathcal{E}_h}\int_e \llbracket\partial_n u_h\rrbracket_e\, (D_{nn}\tilde{u} - \tilde{\sigma}^{\mathrm{eq}}_{h,nn})\,\mathrm{d}s.
\end{aligned} \tag{4.10}$$

Introducing the equilibrated moment tensor of the normal direction in the last term of (4.7), we have

$$\begin{aligned}
\sum_{e\in\mathcal{E}_h}\int_e \llbracket u_h\rrbracket_e \operatorname{div}(D^2\tilde{u})\cdot\boldsymbol{n}_e\,\mathrm{d}s &= \sum_{e\in\mathcal{E}_h}\int_e \llbracket u_h\rrbracket_e \operatorname{div}\underline{\underline{\tilde{\boldsymbol{\sigma}}}}_h^{\mathrm{eq}}\cdot\boldsymbol{n}_e\,\mathrm{d}s\\
&\quad + \sum_{e\in\mathcal{E}_h}\int_e \llbracket\partial_n u_h\rrbracket_e (\operatorname{div}(D^2\tilde{u}) - \operatorname{div}\underline{\underline{\tilde{\boldsymbol{\sigma}}}}_h^{\mathrm{eq}})\cdot\boldsymbol{n}_e\,\mathrm{d}s.
\end{aligned} \tag{4.11}$$

The last five displayed equations (4.7)-(4.11) represent the goal error equation (4.2) with the estimator term $\eta^{\mathrm{res}}_{h,\mathrm{goal}}(u_h,\tilde{u}_h;\underline{\underline{\boldsymbol{\sigma}}}_h^{\mathrm{eq}},\underline{\underline{\tilde{\boldsymbol{\sigma}}}}_h^{\mathrm{eq}})$ and remainder term $\mathcal{R}^{\mathrm{res}}_{h,\mathrm{rem}}(u,\tilde{u},f;u_h,\tilde{u}_h)$. □

We often suppress the dependent variables for the goal estimator and remainder terms for the simplicity of notation. The residual-based a posteriori estimator $\eta^{\mathrm{res}}_{h,\mathrm{goal}}$ in the above Theorem 4.1 provides an estimator for the approximation $Q(u_h)$ of the goal functional $Q(u)$ with a remainder term $\mathcal{R}^{\mathrm{res}}_{h,\mathrm{rem}}$. The estimator is computed using the approximations u_h of the primal and $\tilde{u}_h$ of the dual problems together with the potential reconstruction $\tilde{s}_h$ of Definition 3.1, and the equilibrated moment tensors $\underline{\underline{\boldsymbol{\sigma}}}_h^{\mathrm{eq}}$ and $\underline{\underline{\tilde{\boldsymbol{\sigma}}}}_h^{\mathrm{eq}}$ of Definition 3.2. The potential reconstruction $\tilde{s}_h$ is used in the above Theorem 4.1 to represent the data oscillation without additional regularity assumption on the given data.

A simplified residual-based goal estimator. If f and $\operatorname{div}\operatorname{div}\underline{\underline{\boldsymbol{\sigma}}}_h^{\mathrm{eq}}$ belong to $L^2(\Omega)$, we can replace $\tilde{s}_h$ by $\tilde{u}_h$ in (4.8) and obtain a simplified estimator of Theorem 4.1 as

$$\begin{aligned}
\eta^{\mathrm{res}}_{h,\mathrm{goal}} &:= (f - \operatorname{div}\operatorname{div}\underline{\underline{\boldsymbol{\sigma}}}_h^{\mathrm{eq}},\tilde{u}_h) + \sum_{K\in\mathcal{T}_h}\int_K (\underline{\underline{\boldsymbol{\sigma}}}_h^{\mathrm{eq}} - D^2u_h) : \underline{\underline{\tilde{\boldsymbol{\sigma}}}}_h^{\mathrm{eq}}\,\mathrm{d}x\\
&\quad + \sum_{e\in\mathcal{E}_h}\int_e \llbracket\partial_\tau u_h\rrbracket_e\, \tilde{\sigma}^{\mathrm{eq}}_{h,n\tau}\,\mathrm{d}s + \sum_{e\in\mathcal{E}_h}\int_e \llbracket\partial_n u_h\rrbracket_e\, \tilde{\sigma}^{\mathrm{eq}}_{h,nn}\,\mathrm{d}s\\
&\quad + \sum_{e\in\mathcal{E}_h}\int_e \llbracket u_h\rrbracket_e \operatorname{div}\underline{\underline{\tilde{\boldsymbol{\sigma}}}}_h^{\mathrm{eq}}\cdot\boldsymbol{n}_e\,\mathrm{d}s,
\end{aligned} \tag{4.12}$$

with remainder term

$$\begin{aligned}
\mathcal{R}^{\mathrm{res}}_{h,\mathrm{rem}} &:= (f - \operatorname{div}\operatorname{div}\underline{\underline{\boldsymbol{\sigma}}}_h^{\mathrm{eq}},\tilde{u}-\tilde{u}_h) + \sum_{K\in\mathcal{T}_h}\int_K (\underline{\underline{\boldsymbol{\sigma}}}_h^{\mathrm{eq}} - D^2u_h) : (D^2\tilde{u} - \underline{\underline{\tilde{\boldsymbol{\sigma}}}}_h^{\mathrm{eq}})\,\mathrm{d}x\\
&\quad + \sum_{e\in\mathcal{E}_h}\int_e \llbracket\partial_\tau u_h\rrbracket_e\, (D^2_{n\tau}\tilde{u} - \tilde{\sigma}^{\mathrm{eq}}_{h,n\tau})\,\mathrm{d}s\\
&\quad + \sum_{e\in\mathcal{E}_h}\int_e \llbracket\partial_n u_h\rrbracket_e\, (D^2_{nn}\tilde{u} - \tilde{\sigma}^{\mathrm{eq}}_{h,nn})\,\mathrm{d}s\\
&\quad + \sum_{e\in\mathcal{E}_h}\int_e \llbracket u_h\rrbracket_e (\operatorname{div}(D^2\tilde{u}) - \operatorname{div}\underline{\underline{\tilde{\boldsymbol{\sigma}}}}_h^{\mathrm{eq}})\cdot\boldsymbol{n}_e\,\mathrm{d}s.
\end{aligned}$$

Localization of the goal estimator. To quantify the distribution of error for the approximation of goal functional in the estimator, we localize the estimator as follows. The estimator $\eta^{\mathrm{res}}_{h,\mathrm{goal}}$ of (4.12) can be expressed as the sum of local element error contributions:

$$\eta^{\mathrm{res}}_{h,\mathrm{goal}} = \sum_{K\in\mathcal{T}_h}\eta_K = \sum_{K\in\mathcal{T}_h}(\eta_{\mathrm{est},K} + \eta_{\mathrm{jump},K} + \eta_{\mathcal{O},K}),$$

where the local contributions are given by

$$\begin{aligned}
\eta_{\mathrm{est},K} &:= \int_K (\underline{\underline{\boldsymbol{\sigma}}}_h^{\mathrm{eq}} - D^2u_h) : \underline{\underline{\tilde{\boldsymbol{\sigma}}}}_h^{\mathrm{eq}}\,\mathrm{d}x,\\
\eta_{\mathrm{jump},K} &:= \sum_{e\in\mathcal{E}_K}\int_e \gamma_e\left(\llbracket\partial_n u_h\rrbracket_e\,\tilde{\sigma}^{\mathrm{eq}}_{h,nn} + \llbracket\partial_\tau u_h\rrbracket_e\,\tilde{\sigma}^{\mathrm{eq}}_{h,n\tau} + \llbracket u_h\rrbracket_e \operatorname{div}\underline{\underline{\tilde{\boldsymbol{\sigma}}}}_h^{\mathrm{eq}}\cdot\boldsymbol{n}_e\right)\mathrm{d}s,\\
\eta_{\mathcal{O},K} &:= \int_K (f - \operatorname{div}\operatorname{div}\underline{\underline{\boldsymbol{\sigma}}}_h^{\mathrm{eq}})\tilde{u}_h\,\mathrm{d}x,
\end{aligned}$$

with the indicator function $\gamma_e = 1/2$ for interior edge $e\in\mathcal{E}_h(\Omega)$ and $\gamma_e = 1$ for boundary edge $e\in\mathcal{E}_h(\partial\Omega)$. These local contributions are useful to design an adaptive algorithm.

4.2. Guaranteed a posteriori error estimate

This subsection presents a guaranteed a posteriori error estimator for the goal error based on the equilibrated moment tensor and the potential reconstruction. An abstract a posteriori estimator is derived. In Section 5, we discuss two different finite element approximations for the practical realisations of the error estimation. Here and throughout this subsection, for given $\underline{\underline{\boldsymbol{\sigma}}}_h^{\mathrm{eq}}$ and $\underline{\underline{\tilde{\boldsymbol{\sigma}}}}_h^{\mathrm{eq}}$ belonging to $[L^2(\Omega)]^{2\times2}_{\mathrm{sym}}$, we define $f_h := \operatorname{div}\operatorname{div}\underline{\underline{\boldsymbol{\sigma}}}_h^{\mathrm{eq}}$ and $\tilde{f}_h := \operatorname{div}\operatorname{div}\underline{\underline{\tilde{\boldsymbol{\sigma}}}}_h^{\mathrm{eq}}$. We proceed first by writing a goal error which is a generalisation of [29, Theorem 4.5] to the fourth-order biharmonic problem as:

Lemma 4.2 *(Goal error equation). Let u and $\tilde{u}\in H^2_0(\Omega)$ respectively be the solution of (3.1) and (3.4). Let u_h and $\tilde{u}_h\in\mathbb{P}_k(\mathcal{T}_h)$ respectively be arbitrary piecewise polynomial approximations for u and $\tilde{u}$. Let s_h be the potential reconstructions of Definition 3.1, and $\underline{\underline{\boldsymbol{\sigma}}}_h^{\mathrm{eq}}$ be the equilibrated moment tensors of Definition 3.2. There holds*

$$Q(u) - Q(u_h) = \langle f - f_h,\tilde{u}\rangle + (\underline{\underline{\boldsymbol{\sigma}}}_h^{\mathrm{eq}} - D^2s_h, D^2\tilde{u}) + Q(s_h - u_h). \tag{4.13}$$

Proof. From the primal dual equivalence relation (4.1) and Definition 3.2, we obtain

$$\begin{aligned}
Q(u) &= \langle f,\tilde{u}\rangle = \langle f - f_h,\tilde{u}\rangle + \langle f_h,\tilde{u}\rangle\\
&= \langle f - f_h,\tilde{u}\rangle + \langle \operatorname{div}\operatorname{div}\underline{\underline{\boldsymbol{\sigma}}}_h^{\mathrm{eq}},\tilde{u}\rangle = \langle f - f_h,\tilde{u}\rangle + (\underline{\underline{\boldsymbol{\sigma}}}_h^{\mathrm{eq}}, D^2\tilde{u}).
\end{aligned}$$

Since $s_h\in H^2_0(\Omega)$, from the weak formulation of dual problem (3.5) with $v = s_h$, we obtain

$$\begin{aligned}
Q(u_h) &= Q(s_h) + Q(u_h - s_h) = (D^2\tilde{u}, D^2s_h) + Q(u_h - s_h)\\
&= (D^2s_h, D^2\tilde{u}) + Q(u_h - s_h).
\end{aligned}$$

From the above two displayed equations, we have

$$Q(u) - Q(u_h) = \langle f - f_h, \tilde{u}\rangle + (\underline{\underline{\sigma}}_h^{\mathrm{eq}} - D^2 s_h, D^2\tilde{u}) - Q(u_h - s_h).$$

This completes the proof. □

We apply the principle of the classical bounding technique of Ladevèze et al. [27,26] related to the goal-oriented a posteriori error estimate of the elasticity problem. Let

$$\tilde{\sigma}_h^{\mathrm{m}} := \frac{1}{2}\left(\tilde{\underline{\underline{\sigma}}}_h^{\mathrm{eq}} + D^2 \tilde{s}_h^i\right) \tag{4.14}$$

be the average of the moment tensor of Definition 3.2 and hessian of the potential reconstruction of Definition 3.1 for the dual problem. We denote the following oscillation terms by

$$osc_{\mathrm{prim}}^2(f,\tilde{u}) := |\langle f - f_h, \tilde{u} - \tilde{s}_h\rangle| \text{ and } osc_{\mathrm{dual}}^2(\tilde{f},\tilde{u}) := |\langle \tilde{f} - \tilde{f}_h, \tilde{u} - \tilde{s}_h\rangle|. \tag{4.15}$$

Theorem 4.3 *(Abstract goal-oriented a posteriori estimator). Let u and $\tilde{u} \in H_0^2(\Omega)$ respectively be the solution of (3.1) and (3.4). Let u_h and $\tilde{u}_h \in \mathbb{P}_k(\mathcal{T}_h)$ respectively be arbitrary piecewise polynomial approximations for u and $\tilde{u}$. Let s_h and $\tilde{s}_h$ be the potential reconstructions of Definition 3.1, and $\underline{\underline{\sigma}}_h^{\mathrm{eq}}$ and $\tilde{\underline{\underline{\sigma}}}_h^{\mathrm{eq}}$ be the equilibrated moment tensors of Definition 3.2 with $\tilde{\sigma}_h^{\mathrm{m}}$ being the average moment tensor of (4.14). There holds*

$$\begin{aligned}
&\left|Q(u) - Q(u_h) - \left(\underline{\underline{\sigma}}_h^{\mathrm{eq}} - D^2 s_h, \tilde{\sigma}_h^{\mathrm{m}}\right)\right| \\
&\le \|D^2 s_h - \underline{\underline{\sigma}}_h^{\mathrm{eq}}\|\left(\frac{1}{2}\|D^2\tilde{s}_h - \tilde{\underline{\underline{\sigma}}}_h^{\mathrm{eq}}\| + osc_{\mathrm{dual}}(\tilde{f},\tilde{u})\right) + |\langle f - f_h, \tilde{s}_h\rangle \\
&\quad + Q(s_h - u_h)| + osc_{\mathrm{prim}}^2(f,\tilde{u}).
\end{aligned} \tag{4.16}$$

Proof. Adding and subtracting the average moment tensor $\tilde{\sigma}_h^{\mathrm{m}}$ in (4.13), we obtain

$$\begin{aligned}
&Q(u) - Q(u_h) - \left(\underline{\underline{\sigma}}_h^{\mathrm{eq}} - D^2 s_h, \tilde{\sigma}_h^{\mathrm{m}}\right) \\
&\quad = \langle f - f_h, \tilde{u}\rangle + (\underline{\underline{\sigma}}_h^{\mathrm{eq}} - D^2 s_h, D^2\tilde{u} - \tilde{\sigma}_h^{\mathrm{m}}) + Q(s_h - u_h).
\end{aligned} \tag{4.17}$$

From the definition of (4.14), we have

$$\begin{aligned}
\|D^2\tilde{u} - \tilde{\sigma}_h^{\mathrm{m}}\|^2 &= \frac{1}{4}\|D^2(\tilde{u} - \tilde{s}_h)\|^2 + \frac{1}{4}\|D^2\tilde{u} - \tilde{\underline{\underline{\sigma}}}_h^{\mathrm{eq}}\|^2 \\
&\quad + \frac{1}{2}(D^2(\tilde{u} - \tilde{s}_h), D^2\tilde{u} - \tilde{\underline{\underline{\sigma}}}_h^{\mathrm{eq}}).
\end{aligned}$$

Apply the integration by parts twice to obtain

$$(D^2(\tilde{u} - \tilde{s}_h), D^2\tilde{u} - \tilde{\underline{\underline{\sigma}}}_h^{\mathrm{eq}}) = \langle \tilde{u} - \tilde{s}_h, \tilde{f} - \tilde{f}_h\rangle.$$

The above two equations and (3.8) with $\tilde{v} = \tilde{s}_h$ imply

$$\begin{aligned}
\|D^2\tilde{u} - \tilde{\sigma}_h^{\mathrm{m}}\|^2 &= \frac{1}{4}\|D^2\tilde{s}_h - \tilde{\underline{\underline{\sigma}}}_h^{\mathrm{eq}}\|^2 + \langle \tilde{u} - \tilde{s}_h, \tilde{f} - \tilde{f}_h\rangle \\
&\le \left(\frac{1}{2}\|D^2\tilde{s}_h - \tilde{\underline{\underline{\sigma}}}_h^{\mathrm{eq}}\| + osc_{\mathrm{dual}}(\tilde{f},\tilde{u})\right)^2.
\end{aligned} \tag{4.18}$$

Apply the Schwarz inequality in the right hand side of (4.17) and use (4.18) to obtain

$$\begin{aligned}
&|Q(u) - Q(u_h) - \left(\underline{\underline{\sigma}}_h^{\mathrm{eq}} - D^2 s_h, \tilde{\sigma}_h^{\mathrm{m}}\right)| \\
&\le \|D^2 s_h - \underline{\underline{\sigma}}_h^{\mathrm{eq}}\|\left(\frac{1}{2}\|D^2\tilde{s}_h - \tilde{\underline{\underline{\sigma}}}_h^{\mathrm{eq}}\| + osc_{\mathrm{dual}}(\tilde{f},\tilde{u})\right) \\
&\quad + |\langle f - f_h, \tilde{u}\rangle + Q(s_h - u_h)| \\
&\le \|D^2 s_h - \underline{\underline{\sigma}}_h^{\mathrm{eq}}\|\left(\frac{1}{2}\|D^2\tilde{s}_h - \tilde{\underline{\underline{\sigma}}}_h^{\mathrm{eq}}\| + osc_{\mathrm{dual}}(\tilde{f},\tilde{u})\right) \\
&\quad + |\langle f - f_h, \tilde{s}_h\rangle + Q(s_h - u_h)| + osc_{\mathrm{prim}}(f,\tilde{u}).
\end{aligned}$$

This completes the proof. □

The above estimator (4.16) incorporates a correction $(\underline{\underline{\sigma}}_h^{\mathrm{eq}} - D^2 s_h, \tilde{\sigma}_h^{\mathrm{m}})$ to the approximation $Q(u_h)$ for the goal functional $Q(u)$. Moreover, the average equilibrated moment tensor $\tilde{\sigma}_h^{\mathrm{m}}$ helps to reduce the effectivity by a factor of $1/2$ on the right hand side of the estimator. The potential reconstructions s_h and $\tilde{s}_h$ of Definition 3.1 are the essential part of the above abstract estimator, and also this helps to represent the data oscillation without additional regularity assumptions on the given data. The essential difference of the above estimator (4.16) from the residual type estimator (6.3) is that it provides a guaranteed upper bound with a correction to the approximation of the goal functional.

Some bounds for the oscillation terms of (4.16). The triangle inequality and Lemma 3.3 imply

$$\|\tilde{u} - \tilde{s}_h\|_2 \le \|\tilde{u} - \hat{\tilde{u}}\|_2 + \|\hat{\tilde{u}} - \tilde{s}_h\|_{2,h} \le \|\tilde{f}_h - \tilde{f}\|_{-2} + \|D^2\tilde{s}_h - \tilde{\underline{\underline{\sigma}}}_h^{\mathrm{eq}}\|.$$

This leads to a bound for the data oscillation defined in (4.15),

$$\begin{aligned}
osc_{\mathrm{dual}}^2(\tilde{f},\tilde{u}) &:= |(\tilde{f} - \tilde{f}_h, \tilde{u} - \tilde{s}_h)| \le \|\tilde{f} - \tilde{f}_h\|_{-2}\|\tilde{u} - \tilde{s}_h\|_2 \\
&\le \|\tilde{f} - \tilde{f}_h\|_{-2}\left(\|\tilde{f} - \tilde{f}_h\|_{-2} + \|D^2\tilde{s}_h - \tilde{\underline{\underline{\sigma}}}_h^{\mathrm{eq}}\|\right).
\end{aligned}$$

Similarly, the second data oscillation in (4.15) can be bounded as

$$osc_{\mathrm{prim}}^2(f,\tilde{u}) \le \|f - f_h\|_{-2}\left(\|\tilde{f} - \tilde{f}_h\|_{-2} + \|D^2\tilde{s}_h - \tilde{\underline{\underline{\sigma}}}_h^{\mathrm{eq}}\|\right). \tag{4.19}$$

We observe that if there are no data oscillations for primal and dual problems, then $osc_{\mathrm{prim}}(\tilde{f},\tilde{u}) = 0$ and $osc_{\mathrm{dual}}(f,\tilde{u}) = 0$. Then the abstract a posteriori estimator (4.16) yields the simplified form:

$$\begin{aligned}
&\left|Q(u) - Q(u_h) - \left(\underline{\underline{\sigma}}_h^{\mathrm{eq}} - D^2 s_h, \tilde{\sigma}_h^{\mathrm{m}}\right)\right| \\
&\quad \le \frac{1}{2}\|D^2 s_h - \underline{\underline{\sigma}}_h^{\mathrm{eq}}\|\|D^2\tilde{s}_h - \tilde{\underline{\underline{\sigma}}}_h^{\mathrm{eq}}\| + |Q(s_h - u_h)|.
\end{aligned}$$

5. Discretization of the biharmonic equation

In this section, two non-conforming finite element methods are discussed to realise the estimator found in Section 4. At first, finite element approximation is introduced, and then some procedures are described to obtain the potential reconstruction of Definition 3.1 and the equilibrated moment tensor of Definition 3.2. Here and for the rest of the article, we assume $f, \tilde{f} \in L^2(\Omega)$ and $k \ge 2$.

5.1. C^0IPDG method

We obtain an approximate solution by the C^0 interior penalty method (C^0IPDG); see [9,18,6]. Define the polynomial space for C^0IPDG by

$$V_h^k := \{v_{\mathrm{IP}} \in C^0(\Omega) \mid v_{\mathrm{IP}}|_K \in \mathbb{P}_k(K),\ K \in \mathcal{T}_h\}.$$

Define the bilinear form $a_{\mathrm{IP}} : V_h^k \times V_h^k \to \mathbb{R}$ by

$$\begin{aligned}
a_{\mathrm{IP}}(u_{\mathrm{IP}}, v_{\mathrm{IP}}) &:= \sum_{K\in\mathcal{T}_h}\int_K D^2 u_{\mathrm{IP}} : D^2 v_{\mathrm{IP}}\,\mathrm{dx} - \sum_{e\in\mathcal{E}_h}\int_e \left[\!\left[\partial_n u_{\mathrm{IP}}\right]\!\right]_e \left\{\!\left\{D^2 v_{\mathrm{IP},nn}\right\}\!\right\}_e \mathrm{ds} \\
&\quad - \sum_{e\in\mathcal{E}_h}\int_e \left\{\!\left\{D^2 u_{\mathrm{IP},nn}\right\}\!\right\}_e \left[\!\left[\partial_n v_{\mathrm{IP}}\right]\!\right]_e \mathrm{ds} \\
&\quad + \sum_{e\in\mathcal{E}_h}\frac{\sigma}{h_e}\int_e \left[\!\left[\partial_n u_{\mathrm{IP}}\right]\!\right]_e \left[\!\left[\partial_n v_{\mathrm{IP}}\right]\!\right]_e \mathrm{ds},
\end{aligned}$$

where σ is large positive penalty parameter. Define the linear forms for the primal and dual problems as

$$l_{\mathrm{IP}}(v_{\mathrm{IP}}) := \sum_{K\in\mathcal{T}_h}\int_K f v_{\mathrm{IP}}\,\mathrm{dx} \text{ and } \tilde{l}_{\mathrm{IP}}(v_{\mathrm{IP}}) := \sum_{K\in\mathcal{T}_h}\int_K \tilde{f} v_{\mathrm{IP}}\,\mathrm{dx} \quad \forall\, v_{\mathrm{IP}} \in V_h^k.$$

The C^0IPDG method for (3.2) seeks $u_{\mathrm{IP}} \in V_h^k$ such that

$$a_{\mathrm{IP}}(u_{\mathrm{IP}}, v_{\mathrm{IP}}) = l_{\mathrm{IP}}(v_{\mathrm{IP}}) \quad \forall\, v_{\mathrm{IP}} \in V_h^k, \tag{5.1}$$

and C^0IPDG method for the dual problem (3.5) seeks $\tilde{u}_{\mathrm{IP}} \in V_h^k$ such that

$$a_{\mathrm{IP}}(\tilde{u}_{\mathrm{IP}}, v_{\mathrm{IP}}) = \tilde{l}_{\mathrm{IP}}(v_{\mathrm{IP}}) \quad \forall\, v_{\mathrm{IP}} \in V_h^k. \tag{5.2}$$

The discretization error is measured by the mesh-dependent norm

$$\|v\|_{\mathrm{IP}}^2 := \sum_{K\in\mathcal{T}_h} \|D^2 v\|_{0,K}^2 + \sum_{e\in\mathcal{E}_h} \frac{\sigma}{h_e} \|[\![\partial_n v]\!]_e\|_{0,e}^2 \quad \forall\, v \in V_h^k + H_0^2(\Omega).$$

It is well known that for sufficiently large $\sigma = O((k+1)^2)$, there exists a positive constant β such that the following coercivity result holds (see [9,18,6]):

$$a_{\mathrm{IP}}(v_{\mathrm{IP}}, v_{\mathrm{IP}}) \geq \beta \|v_{\mathrm{IP}}\|_{\mathrm{IP}}^2 \quad \forall\, v_{\mathrm{IP}} \in V_h^k.$$

Also, the bilinear form $a_{\mathrm{IP}}(\bullet,\bullet)$ is continuous, i.e., $|a_{\mathrm{IP}}(v,w)| \leq C\|v\|_{\mathrm{IP}}\|w\|_{\mathrm{IP}}$ for all $v, w \in V_h^k$. The boundedness and coercivity of $a_{\mathrm{IP}}(\bullet,\bullet)$, and continuity of l_{IP} and $\tilde{l}_{\mathrm{IP}}$ lead to the existence and uniqueness of the solution of primal and dual problems (5.1)-(5.2) by the Lax-Milgram lemma.

The estimator of Theorem 4.1 is computed by the construction of equilibrated moment tensors $\underline{\underline{\boldsymbol{\sigma}}}_h^{\mathrm{eq}}$ and $\underline{\underline{\tilde{\boldsymbol{\sigma}}}}_h^{\mathrm{eq}}$ of Definition 3.2, and potential reconstructions s_h and $\tilde{s}_h$ of Definition 3.1. Their constructions are outlined below:

Construction of equilibrated moment tensor. We follow [6] for the construction of an equilibrated moment tensor. Define the symmetric piecewise polynomial tensor fields of order $k-1$ with the continuous normal-normal component $\underline{\underline{\boldsymbol{\tau}}}_{h,nn} = \boldsymbol{n}_e^T \underline{\underline{\boldsymbol{\tau}}}_h \boldsymbol{n}_e$ by

$$\underline{\underline{\mathbf{M}}}_h^{\mathrm{eq}} := \{\underline{\underline{\boldsymbol{\tau}}}_h \in [L^2(\Omega)]_{\mathrm{sym}}^{2\times 2} \mid \underline{\underline{\boldsymbol{\tau}}}_h \in [\mathbb{P}_{k-1}(K)]_{\mathrm{sym}}^{2\times 2}, K \in \mathcal{T}_h, \underline{\underline{\boldsymbol{\tau}}}_{h,nn} \text{ is continuous at interelement boundaries}\}.$$

Each $\underline{\underline{\boldsymbol{\tau}}}_h \in \underline{\underline{\mathbf{M}}}_h^{\mathrm{eq}}$ is uniquely defined by the degrees of freedom (see [15, 6])

$$\int_e \underline{\underline{\boldsymbol{\tau}}}_{h,nn} q_e \,\mathrm{ds}, \quad q_e \in \mathbb{P}_{k-1}(e), e \in \mathcal{E}_h(K),$$

$$\int_K \underline{\underline{\boldsymbol{\tau}}}_h : q_K \,\mathrm{dx}, \quad q_K \in [P_{k-2}(K)]_{\mathrm{sym}}^{2\times 2}, K \in \mathcal{T}_h.$$

This leads to the construction of an equilibrated moment tensor:

Lemma 5.1. *[6, Lemma 5.1] There exists unique equilibrated moment tensor $\underline{\underline{\boldsymbol{\sigma}}}_h^{\mathrm{eq}} \in \underline{\underline{\mathbf{M}}}_h^{\mathrm{eq}}$ such that for each $K \in \mathcal{T}_h$,*

$$\sigma_{h,nn}^{\mathrm{eq}} = \{\{D^2 u_{\mathrm{IP},nn}\}\}_e - \frac{\sigma}{h_e}[\![\partial_n u_{\mathrm{IP}}]\!]_e \quad \in \mathbb{P}_{k-1}(e), e \in \mathcal{E}_h(K),$$

$$\int_K \underline{\underline{\boldsymbol{\sigma}}}_h^{\mathrm{eq}} : q_K \,\mathrm{dx} = \int_K D^2 u_{\mathrm{IP}} : q_K \,\mathrm{dx} - \sum_{e\subset\mathcal{E}_h(K)} \int_e \gamma_e [\![\partial_n u_{\mathrm{IP}}]\!]_e q_{K,nn} \,\mathrm{ds} \quad \forall\, q_K \in [P_{k-2}(K)]_{\mathrm{sym}}^{2\times 2},$$

where $\gamma_e = 1/2$ for interior edge $e \in \mathcal{E}_h(\Omega)$ and $\gamma_e = 1$ for a boundary edge $e \in \mathcal{E}_h(\partial\Omega)$. Moreover, the equilibrated moment tensor satisfies [6, eq. (5.6)]

$$\langle \mathrm{div}\,\mathrm{div}\, \underline{\underline{\boldsymbol{\sigma}}}_h^{\mathrm{eq}}, v_{\mathrm{IP}}\rangle = (f, v_{\mathrm{IP}}) \quad \forall\, v_{\mathrm{IP}} \in V_h^k. \tag{5.3}$$

By the above Lemma 5.1 and following [6], we have the efficiency result:

Lemma 5.2. *Let u_{IP} be the discrete solution of (5.1) and $\underline{\underline{\boldsymbol{\sigma}}}_h^{\mathrm{eq}}$ be of (5.3). Then the following efficiency result holds:*

$$\|\underline{\underline{\boldsymbol{\sigma}}}_h^{\mathrm{eq}} - D^2 u_{\mathrm{IP}}\|^2 \lesssim \|u - u_{\mathrm{IP}}\|_{\mathrm{IP}}^2 + \sum_{K\in\mathcal{T}_h} h_K^4 \|f - \bar{f}\|_{L^2(K)}^2,$$

where $\bar{f}$ is any interpolation of f into the space of piecewise polynomial functions of total degree less than equals to k.

Computation of potential reconstruction. We describe the construction of a potential reconstruction for $k=2$ by averaging [7,14,8]: let $\bar{V}_h \subset H_0^2(\Omega)$ be the Hsieh–Clough–Tocher associated with the triangulation $\mathcal{T}_h$. For higher-degree approximations $k \geq 3$, we refer [20] for an extension of this approach, see also (5.11) below. We define the enrichment operator $E_h : V_h^k \to \bar{V}_h$ as follows: let N be any (global) degree of freedom of $\bar{V}_h$, i.e., N is either the evaluation of a shape function or its first-order derivatives at an interior vertex of $\mathcal{T}_h$ or the evaluation of the normal derivative of a shape function at the midpoint of an interior edge. For $v_{\mathrm{IP}} \in V_h^k$ define

$$N(E_h v_{\mathrm{IP}}) = \frac{1}{|\mathcal{T}_N|} \sum_{K\in\mathcal{T}_N} N(v_{\mathrm{IP}}|_K) \tag{5.4}$$

where $\mathcal{T}_N$ is the set of triangles in $\mathcal{T}_h$ that share the degree of freedom N and $|\mathcal{T}_N|$ is the number of elements of $\mathcal{T}_N$. The enrichment operator satisfies the estimate:

$$\|E_h v_{\mathrm{IP}} - v_{\mathrm{IP}}\|_{\mathrm{IP}} \leq C \inf_{v\in H_0^2(\Omega)} \|v - v_{\mathrm{IP}}\|_{\mathrm{IP}}, \tag{5.5}$$

for some positive constant C. Finally, we set $s_h := E_h u_{\mathrm{IP}}$ and $\tilde{s}_h := E_h \tilde{u}_{\mathrm{IP}}$ to compute the estimator in (4.16). Moreover, the efficiency $\|s_h - u_{\mathrm{IP}}\|_{\mathrm{IP}} \leq C\|u - u_{\mathrm{IP}}\|_{\mathrm{IP}}$ follows from (5.5) with $v_{\mathrm{IP}} = u_{\mathrm{IP}}$ and the choice $v = u$.

Computation of data oscillation. We follow the procedure of [6, Lemma 6.1] to compute the oscillation of data f and $\tilde{f}$. Assume the data f and $\tilde{f}$ belong to $L^2(\Omega)$. Let $\bar{f}$ denote the L^2 projection of f onto the (discontinuous) space of piecewise polynomials of degree $k-3$ in $\mathcal{T}_h$. Then the oscillation can be bounded by

$$\|f - f_h\|_{-2} \leq c \left(\sum_{K\in\mathcal{T}_h} h_K^4 \|f - \bar{f}\|_{0,K}^2\right)^{1/2} \text{ and}$$

$$\|\tilde{f} - \tilde{f}_h\|_{-2} \leq c \left(\sum_{K\in\mathcal{T}_h} h_K^4 \|\tilde{f} - \bar{\tilde{f}}\|_{0,K}^2\right)^{1/2},$$

where the constant c is independent of h but depends on the shape-regularity of the mesh. In the case of $k=2$, the projections can be set as $\bar{f} = 0$ and $\bar{\tilde{f}} = 0$.

We state convergence result, see [9,7,24]:

$$\|u - u_{\mathrm{IP}}\|_h \leq \left(\inf_{v_{\mathrm{IP}}\in V_h^k} \|u - v_{\mathrm{IP}}\|_h + osc_2(f)\right)$$

where, the norm is defined by $\|v_{\mathrm{IP}}\|_h^2 := \|v_{\mathrm{IP}}\|_{\mathrm{IP}}^2 + \sum_{e\in\mathcal{E}_h}\sum_{i,j=1,2} \left\|\left\{\left\{\frac{\partial^2 v_{\mathrm{IP}}}{\partial x_i \partial x_j}\right\}\right\}_e\right\|_{L^2(e)}^2$ and the data oscillation by

$$osc_2(f) := \left(\sum_{K\in\mathcal{T}_h} h_K^4 \inf_{\bar{f}\in P_{k-2}(K)} \|f - \bar{f}\|_{L^2(K)}^2\right)^{1/2}.$$

This is used to obtain a convergence result for the goal error as follows.

For the above C^0IPDG approximation, we observe that $[\![u_{\mathrm{IP}}]\!]_e = 0 = [\![\partial_\tau u_{\mathrm{IP}}]\!]_e$. This is used to simplify the goal residual estimator of (4.3) as follows:

$$\eta_{h,\mathrm{goal}}^{\mathrm{res}} := (f - \mathrm{div}\,\mathrm{div}\, \underline{\underline{\boldsymbol{\sigma}}}_h^{\mathrm{eq}}, \tilde{u}_{\mathrm{IP}}) + \sum_{K\in\mathcal{T}_h} \int_K (\underline{\underline{\boldsymbol{\sigma}}}_h^{\mathrm{eq}} - D^2 u_{\mathrm{IP}}) : \underline{\underline{\tilde{\boldsymbol{\sigma}}}}_h^{\mathrm{eq}} \,\mathrm{dx} + \sum_{e\in\mathcal{E}_h} \int_e [\![\partial_n u_{\mathrm{IP}}]\!]_e \tilde{\sigma}_{h,nn}^{\mathrm{eq}} \,\mathrm{ds}. \tag{5.6}$$

Moreover, the remainder term has the estimate:

Theorem 5.3. *Let u and $\tilde{u} \in H_0^2(\Omega)$ respectively be the solution of (3.2) and (3.5). Let $u_{\mathrm{IP}} \in V_h^k$ and $\tilde{u}_{\mathrm{IP}} \in V_h^m$ respectively be the solution of (5.1) and (5.2). Assume $\|u - u_{\mathrm{IP}}\|_{\mathrm{IP}}$ and $\|\tilde{u} - \tilde{u}_{\mathrm{IP}}\|_{\mathrm{IP}}$, respectively, converge with orders $O(h^k)$ and $O(h^m)$. Then the remainder term $\mathcal{R}^{\mathrm{res}}_{h,\mathrm{rem}}$ of (4.4) has the convergence*

$$|\mathcal{R}^{\mathrm{res}}_{h,\mathrm{rem}}(u,\tilde{u},f;u_{\mathrm{IP}},\tilde{u}_{\mathrm{IP}})| \le Ch^{k+m}, \tag{5.7}$$

where the positive constant C (independent of the mesh parameter h) depends on the load function f, and the exact solutions u and $\tilde{u}$.

Proof. Recall the remainder term $\mathcal{R}^{\mathrm{res}}_{h,\mathrm{rem}}(u,\tilde{u},f;u_{\mathrm{IP}},\tilde{u}_{\mathrm{IP}})$ of (4.4)

$$\begin{aligned}\mathcal{R}^{\mathrm{res}}_{h,\mathrm{rem}}(u,\tilde{u},f;u_{\mathrm{IP}},\tilde{u}_{\mathrm{IP}}) &= \langle f - f_h, \tilde{u} - \tilde{s}_h\rangle \\ &\quad + \sum_{K\in\mathcal{T}_h}\int_K (\underline{\underline{\sigma}}_h^{\mathrm{eq}} - D^2u_{\mathrm{IP}}) : (D^2\tilde{u} - \underline{\underline{\tilde{\sigma}}}_h^{\mathrm{eq}})\,\mathrm{dx} \\ &\quad + \sum_{e\in\mathcal{E}_h}\int_e \left[\!\left[\partial_n u_{\mathrm{IP}}\right]\!\right]_e (D^2_{nn}\tilde{u} - \tilde{\sigma}^{\mathrm{eq}}_{h,nn})\,\mathrm{ds}. \end{aligned}\tag{5.8}$$

The first oscillation term in the above (5.8) is estimated by (4.19) as

$$|\langle f - f_h, \tilde{u} - \tilde{s}_h\rangle| \le \|f - f_h\|_{-2}(\|\tilde{f} - \tilde{f}_h\|_{-2} + \|D^2\tilde{s}_h - \underline{\underline{\tilde{\sigma}}}_h^{\mathrm{eq}}\|).$$

The identity (3.8) with $\tilde{v} = \tilde{s}_h$ yields $\|D^2\tilde{u} - \underline{\underline{\tilde{\sigma}}}_h^{\mathrm{eq}}\| \le \|D^2\tilde{s}_h - \underline{\underline{\tilde{\sigma}}}_h^{\mathrm{eq}}\| + \sqrt{2}\,osc_{\mathrm{dual}}(\tilde{f},\tilde{u})$ by the Schwarz inequality. This leads to an estimate for the second term in (5.8) as

$$\begin{aligned}&\sum_{K\in\mathcal{T}_h}\int_K (\underline{\underline{\sigma}}_h^{\mathrm{eq}} - D^2u_{\mathrm{IP}}) : (D^2\tilde{u} - \underline{\underline{\tilde{\sigma}}}_h^{\mathrm{eq}})\,\mathrm{dx} \le \|\underline{\underline{\sigma}}_h^{\mathrm{eq}} - D^2u_{\mathrm{IP}}\|\,\|D^2\tilde{u} - \underline{\underline{\tilde{\sigma}}}_h^{\mathrm{eq}}\| \\ &\quad \le \|\underline{\underline{\sigma}}_h^{\mathrm{eq}} - D^2u_{\mathrm{IP}}\|\left(\|D^2\tilde{s}_h - \underline{\underline{\tilde{\sigma}}}_h^{\mathrm{eq}}\| + \sqrt{2}\,osc_{\mathrm{dual}}(\tilde{f},\tilde{u})\right).\end{aligned}$$

The last term of (5.8) is bounded by the Cauchy–Schwarz inequality

$$\begin{aligned}&\left|\sum_{e\in\mathcal{E}_h}\int_e \left[\!\left[\partial_n u_{\mathrm{IP}}\right]\!\right]_e (D^2_{nn}\tilde{u} - \tilde{\sigma}^{\mathrm{eq}}_{h,nn})\,\mathrm{ds}\right| \\ &\quad \le \sum_{e\in\mathcal{E}_h}\|h_e^{-1/2}\left[\!\left[\partial_n u_{\mathrm{IP}}\right]\!\right]_e\|_{L^2(e)}\|h_e^{1/2}(D^2_{nn}\tilde{u} - \tilde{\sigma}^{\mathrm{eq}}_{h,nn})\|_{L^2(e)} \\ &\quad \le \|u - u_{\mathrm{IP}}\|_{\mathrm{IP}}\left(\sum_{e\in\mathcal{E}_h}\|h_e^{1/2}(D^2_{nn}\tilde{u} - \tilde{\sigma}^{\mathrm{eq}}_{h,nn})\|^2_{L^2(e)}\right)^{1/2}.\end{aligned}$$

The addition and subtraction of u_{IP} with the trace inequality yield

$$\begin{aligned}&\sum_{e\in\mathcal{E}_h}\|h_e^{1/2}(D^2_{nn}\tilde{u} - \tilde{\sigma}^{\mathrm{eq}}_{h,nn})\|^2_{L^2(e)} \\ &\quad \le \sum_{e\in\mathcal{E}_h}\|h_e^{1/2}D^2_{nn}(\tilde{u} - \tilde{u}_{\mathrm{IP}})\|^2_{L^2(e)} + \sum_{e\in\mathcal{E}_h}\|h_e^{1/2}(D^2_{nn}\tilde{u}_{\mathrm{IP}} - \tilde{\sigma}^{\mathrm{eq}}_{h,nn})\|^2_{L^2(e)} \\ &\quad \le \|\tilde{u} - \tilde{u}_{\mathrm{IP}}\|_h + \|D^2\tilde{u}_{\mathrm{IP}} - \underline{\underline{\tilde{\sigma}}}_h^{\mathrm{eq}}\|.\end{aligned}$$

The above displayed estimates and the efficiency result of Lemma 5.2 for primal and dual problems yield the required estimate (5.7). □

Corollary 5.4. *If the primal and dual solutions, respectively u and $\tilde{u}$ belong to $H^{2+\alpha}(\Omega)\cap H_0^2(\Omega)$ for $\frac{1}{2} < \alpha \le 1$, then the remainder estimator $\mathcal{R}^{\mathrm{res}}_{h,\mathrm{rem}}$ of (4.4) has the convergence*

$$|\mathcal{R}^{\mathrm{res}}_{h,\mathrm{rem}}(u,\tilde{u},f;u_{\mathrm{IP}},\tilde{u}_{\mathrm{IP}})| \le Ch^{2\alpha},$$

where the positive constant C (independent of the mesh parameter h) depends on load function f, and exact solutions u and $\tilde{u}$.

5.2. Discontinuous Galerkin FEMs

Let $V_h^k := \mathbb{P}_k(\mathcal{T}_h)$. Define the bilinear form $a_{\mathrm{dG}} : V_h^k \times V_h^k \to \mathbb{R}$ by [5]

$$\begin{aligned}a_{\mathrm{dG}}(u_{\mathrm{dG}},v_{\mathrm{dG}}) &:= \sum_{K\in\mathcal{T}_h}\int_K D^2u_{\mathrm{dG}} : D^2v_{\mathrm{dG}}\,\mathrm{dx} \\ &\quad - \sum_{e\in\mathcal{E}_h}\int_e \left[\!\left[\nabla u_{\mathrm{dG}}\right]\!\right]_e \cdot \{\!\{D^2v_{\mathrm{dG}}\boldsymbol{n}_e\}\!\}_e\,\mathrm{ds} \\ &\quad - \sum_{e\in\mathcal{E}_h}\int_e \{\!\{D^2u_{\mathrm{dG}}\boldsymbol{n}_e\}\!\}_e \cdot \left[\!\left[\nabla v_{\mathrm{dG}}\right]\!\right]_e\,\mathrm{ds} \\ &\quad + \sum_{e\in\mathcal{E}_h}\int_e \left(\left[\!\left[u_{\mathrm{dG}}\right]\!\right]_e \{\!\{\mathrm{div}\,(D^2v_{\mathrm{dG}})\cdot\boldsymbol{n}_e\}\!\}_e\right. \\ &\quad \left. + \{\!\{\mathrm{div}\,(D^2u_{\mathrm{dG}})\cdot\boldsymbol{n}_e\}\!\}_e \left[\!\left[v_{\mathrm{dG}}\right]\!\right]_e\right)\mathrm{ds} \\ &\quad + \sum_{e\in\mathcal{E}_h}\frac{\sigma_1}{h_e}\int_e \left[\!\left[\partial_n u_{\mathrm{dG}}\right]\!\right]_e \left[\!\left[\partial_n v_{\mathrm{dG}}\right]\!\right]_e\,\mathrm{ds} \\ &\quad + \sum_{e\in\mathcal{E}_h}\frac{\sigma_2}{h_e^3}\int_e \left[\!\left[u_{\mathrm{dG}}\right]\!\right]_e \left[\!\left[v_{\mathrm{dG}}\right]\!\right]_e\,\mathrm{ds}\end{aligned}$$

for positive penalty parameters σ_1 and σ_2, and the linear forms

$$l_{\mathrm{dG}}(v_{\mathrm{dG}}) := \sum_{K\in\mathcal{T}_h}\int_K f v_{\mathrm{dG}}\,\mathrm{dx} \text{ and } \tilde{l}_{\mathrm{dG}}(v_{\mathrm{dG}}) := \sum_{K\in\mathcal{T}_h}\int_K \tilde{f} v_{\mathrm{dG}}\,\mathrm{dx}.$$

The DG method for (3.2) seeks $u_{\mathrm{dG}} \in V_h^k$ such that

$$a_{\mathrm{dG}}(u_{\mathrm{dG}},v_{\mathrm{dG}}) = l_{\mathrm{dG}}(v_{\mathrm{dG}}) \quad \forall\, v_{\mathrm{dG}} \in V_h^k, \tag{5.9}$$

and for the dual problem (3.5) seeks $\tilde{u}_{\mathrm{dG}} \in V_h^k$ such that

$$a_{\mathrm{dG}}(\tilde{u}_{\mathrm{dG}},v_{\mathrm{dG}}) = \tilde{l}_{\mathrm{dG}}(v_{\mathrm{dG}}) \quad \forall\, v_{\mathrm{dG}} \in V_h^k. \tag{5.10}$$

The discretization error will be measured by the mesh-dependent dG norm

$$\begin{aligned}\|v\|^2_{\mathrm{dG}} &:= \sum_{K\in\mathcal{T}_h}\|D^2v\|^2_{0,K} + \sum_{e\in\mathcal{E}_h}\frac{\sigma_1}{h_e}\|\left[\!\left[\partial_n v\right]\!\right]_e\|^2_{0,e} \\ &\quad + \sum_{e\in\mathcal{E}_h}\frac{\sigma_2}{h_e^3}\|\left[\!\left[v\right]\!\right]_e\|^2_{0,e} \quad \forall\, v \in V_h^k + H_0^2(\Omega).\end{aligned}$$

It is well known that for sufficiently large $\sigma_1 = O((k+1)^2)$ and $\sigma_2 = O((k+1)^6)$, there exists a positive constant β such that the following coercivity result holds [5]:

$$a_{\mathrm{dG}}(v_{\mathrm{dG}},v_{\mathrm{dG}}) \ge \beta\|v_{\mathrm{dG}}\|^2_{\mathrm{dG}} \quad \forall\, v_{\mathrm{dG}} \in V_h^k.$$

The boundedness $|a_{\mathrm{dG}}(v_{\mathrm{dG}},w_{\mathrm{dG}})| \le C\|v_{\mathrm{dG}}\|_{\mathrm{dG}}\|w_{\mathrm{dG}}\|_{\mathrm{dG}}$ for all $v_{\mathrm{dG}}, w_{\mathrm{dG}} \in V_{\mathrm{dG}}$ also holds. Then, the existence and uniqueness of the solution of the primal and the dual problems (5.9)-(5.10) follow from the Lax-Milgram lemma. Moreover, one can extend the definition of $a_{\mathrm{dG}}(\bullet,\bullet)$ to $V_h^k + H_0^2(\Omega)$ by a lifting operator, see [19], and have the coercivity and boundedness of the extension. An abuse of notation, we also denote the extension of $a_{\mathrm{dG}}(\bullet,\bullet)$ to $V_h^k + H_0^2(\Omega)$ by itself.

Construction of equilibrated moment tensor. We follow [5] to construct an equilibrated moment tensor. The equilibrated moment tensors are constructed in the discrete space $\underline{\underline{\mathbf{M}}}_h^{\mathrm{eq}}$ defined by

$$\underline{\underline{\mathbf{M}}}_h^{\mathrm{eq}} := \left\{\underline{\underline{\tau}}_h \in L^2(\Omega)^{2\times 2} \mid \underline{\underline{\tau}}_h|_K \in P_\ell(K)^{2\times 2}, K\in\mathcal{T}_h\right\} \cap \mathbf{H}(\mathrm{div}^2,\Omega),$$

where $\ell := \begin{cases} k & \text{if } k \ge 3, \\ 3 & \text{if } k = 2. \end{cases}$

For $K \in \mathcal{T}_h$, let f_K be the L^2-projection of f onto $P_{l-2}(K)$, and let $f_h \in L^2(\Omega)$ be such that $f_h|_K = f_K, K \in \mathcal{T}_h$. Let $\mathbf{BDM}_m(K), m \in \mathbb{N}$ be denoted by the Brezzi–Douglas–Marini element of polynomial degree m, see [10]. The construction of an equilibrated moment tensor is obtained in two steps: first, construct an auxiliary vector field $\underline{\boldsymbol{\psi}}_h^{\mathrm{eq}} \in \mathbf{H}(\mathrm{div},\Omega)$, $\underline{\boldsymbol{\psi}}_h^{\mathrm{eq}}|_K \in \mathbf{BDM}_{\ell-1}(K), K \in \mathcal{T}_h$ satisfying

$$\nabla\cdot\underline{\boldsymbol{\psi}}_h^{\mathrm{eq}} = f_h \quad \text{in } L^2(\Omega),$$

and then an equilibrated moment tensor $\underline{\underline{\boldsymbol{\sigma}}}_h^{\mathrm{eq}} \in \underline{\underline{\mathbf{M}}}_h^{\mathrm{eq}}$ satisfying

$$\nabla\cdot\underline{\underline{\boldsymbol{\sigma}}}_h^{\mathrm{eq}} = \underline{\boldsymbol{\psi}}_h^{\mathrm{eq}} \quad \text{in } L^2(\Omega).$$

Define some auxiliary numerical flux functions on the edges $e \in \mathcal{E}_h$ by

$$\widehat{\underline{\boldsymbol{u}}}^{(1)} := \begin{cases} \{\nabla u_h\}_e, & e \in \mathcal{E}_h(\Omega) \\ 0, & e \in \mathcal{E}_h(\partial\Omega), \end{cases}$$

$$\widehat{\underline{u}}^{(2)} := \begin{cases} \{u_h\}_e, & e \in \mathcal{E}_h(\Omega) \\ 0, & e \in \mathcal{E}_h(\partial\Omega), \end{cases}$$

$$\widehat{\underline{\underline{\boldsymbol{p}}}} := \{\{D^2 u_h\}\}_e - \frac{\sigma_1}{h_e}\boldsymbol{n}_e \llbracket \nabla u_h \rrbracket_e^T,$$

$$\widehat{\underline{\boldsymbol{\psi}}} := \{\{\nabla\cdot D^2 u_h\}\}_e + \frac{\sigma_2}{h_e^3}\llbracket u_h \rrbracket_e \boldsymbol{n}_e.$$

The auxiliary vector field $\underline{\boldsymbol{\psi}}_h^{\mathrm{eq}}$ is constructed locally on each element $K \in \mathcal{T}_h$ such that $\underline{\boldsymbol{\psi}}_h^{\mathrm{eq}} \in \mathbf{BDM}_{\ell-1}(K)$ satisfies the following interpolation conditions, see [5, Eq. 6.5]

$$\int_e \boldsymbol{n}_e\cdot\underline{\boldsymbol{\psi}}_h^{\mathrm{eq}}\, q\,\mathrm{d}s = \int_e \boldsymbol{n}_e\cdot\widehat{\underline{\boldsymbol{\psi}}}\, q\,\mathrm{d}s, \quad q \in P_{\ell-1}(e),\ e \in \mathcal{E}_h(\partial K),$$

$$\int_K \underline{\boldsymbol{\psi}}_h^{\mathrm{eq}}\cdot\nabla q\,\mathrm{d}x = \int_{\partial K}\boldsymbol{n}_{\partial K}\cdot\widehat{\underline{\boldsymbol{\psi}}} q\,\mathrm{d}s - \int_K f q\,\mathrm{d}x, \quad q \in P_{\ell-2}(K),$$

$$\int_K \underline{\boldsymbol{\psi}}_h^{\mathrm{eq}}\cdot\mathbf{curl}(b_K q)\,\mathrm{d}x = \int_K (\nabla\cdot D^2 u_h)\cdot\mathbf{curl}(b_K q)\,\mathrm{d}x, \quad q \in P_{\ell-3}(K),$$

where $b_K = \lambda_1^K\lambda_2^K\lambda_3^K$ is the bubble function on element K for barycentric coordinates $\lambda_i^K, i = 1,2,3$ of K and $\mathbf{curl}(\bullet) := (-\partial(\bullet)/\partial y, \partial(\bullet)/\partial x)$. Finally, the equilibrated moment tensor $\underline{\underline{\boldsymbol{\sigma}}}_h^{\mathrm{eq}} = (\sigma_{ij}^{h,\mathrm{eq}})_{i,j=1}^2 \in \underline{\underline{\mathbf{M}}}_h^{\mathrm{eq}}$, with $\underline{\boldsymbol{\sigma}}_{h,\mathrm{eq}}^{(i)} = (\sigma_{i1}^{h,\mathrm{eq}}, \sigma_{i2}^{h,\mathrm{eq}})^T$, $1 \le i \le 2$, in each element K is constructed by fixing the degrees of freedom [5, Eq. 6.8]:

$$\int_e \underline{\underline{\boldsymbol{\sigma}}}_h^{\mathrm{eq}}\boldsymbol{n}_e\cdot\underline{\boldsymbol{q}}\,\mathrm{d}s = \int_e \underline{\underline{\widehat{\boldsymbol{p}}}}\boldsymbol{n}_e\cdot\underline{\boldsymbol{q}}\,\mathrm{d}s, \quad \underline{\boldsymbol{q}} \in [P_\ell(e)]^2,\ e \in \mathcal{E}_h(\partial K),$$

$$\int_K \underline{\underline{\boldsymbol{\sigma}}}_h^{\mathrm{eq}} : \nabla\underline{\boldsymbol{q}}\,\mathrm{d}x = -\int_K \underline{\boldsymbol{\psi}}_h^{\mathrm{eq}}\cdot\underline{\boldsymbol{q}}\,\mathrm{d}x + \int_{\partial K}\underline{\underline{\widehat{\boldsymbol{p}}}}\boldsymbol{n}_{\partial K}\cdot\underline{\boldsymbol{q}}\,\mathrm{d}x, \quad \underline{\boldsymbol{q}} \in [P_{\ell-1}(K)]^2 \setminus [P_0(K)]^2,$$

$$\int_K \underline{\boldsymbol{\sigma}}_{h,\mathrm{eq}}^{(i)}\cdot\mathbf{curl}(b_K q)\,\mathrm{d}x = \int_K \underline{\boldsymbol{z}}^{(i)}\cdot\mathbf{curl}(b_K q)\,\mathrm{d}x, \quad q \in P_{\ell-2}(K), 1 \le i \le 2,$$

where $\underline{\boldsymbol{z}}^{(i)} = (\frac{\partial^2 u_h}{\partial x_i \partial x_1}, \frac{\partial^2 u_h}{\partial x_i \partial x_2}), i = 1,2$. The above constructions lead to the equilibrium: $\mathrm{div}\,\mathrm{div}\,\underline{\underline{\boldsymbol{\sigma}}}_h^{\mathrm{eq}} = f_h$, see [5, Lemma 6.1 & Theorem 6.6]. Similar construction for the dual problem with data $\tilde{f}$ and approximation $\tilde{u}_h$ leads to the equilibrated moment tensor $\underline{\underline{\tilde{\boldsymbol{\sigma}}}}_h^{\mathrm{eq}}$.

Computation of potential reconstruction. Let S_h^r be a C^1-conforming finite-element space consisting of the macro-elements of order $r \ge 4$, see [20, Definition 3.1]. We follow the construction of the recovery operator of [20]. For each nodal point ν of the C^1-conforming finite-element space S_h^{k+2}, define ω_ν to be the set of $K \in \mathcal{T}_h$ that share the nodal point ν, i.e., $\omega_\nu = \{K \in \mathcal{T}_h : \nu \in K\}$. Define the operator $E_h : \mathbb{P}_k(\mathcal{T}_h) \to S_h^{k+2} \cap H_0^2(\Omega)$ by the averaging:

$$N_\nu(E_h v_{\mathrm{dG}}) = \begin{cases} \frac{1}{|\omega_\nu|}\sum_{K\in\omega_\nu} N_\nu(v_{\mathrm{dG}}|_K) & \text{if } \nu \notin \partial\Omega, \\ 0 & \text{if } \nu \in \partial\Omega, \end{cases}$$

where N_ν is any nodal variable at ν and ν is any nodal point of S_h^{k+2}. This operator satisfies the estimate [20, Lemma 3.1] and [12, Lemma 3.5]:

$$\|E_h v_{\mathrm{dG}} - v_{\mathrm{dG}}\|_{\mathrm{dG}} \le C \inf_{v\in H_0^2(\Omega)} \|v - v_{\mathrm{dG}}\|_{\mathrm{dG}}, \tag{5.11}$$

for some positive constant C.

Algorithm 1 Goal-oriented adaptive method. For newest vertex bisection method see [38].

Input: Initial mesh $\mathcal{T}_0$, $J \ge 1$ the maximum number of mesh refinement levels, and real parameter $\theta \in (0,1)$.

Set $j = 0$.
While $(j \le J)$ do

- **SOLVE/COMPUTE**:
  1. Solve the *primal and dual matrix systems* $\mathbb{A}\mathbb{U}_j = \mathbb{F}_j$ and $\mathbb{A}\tilde{\mathbb{U}}_j = \tilde{\mathbb{F}}_j$ related to the discrete problems.
  2. Compute the potential reconstructions s_j for the primal problem and $\tilde{s}_j$ for the dual problem from Definition 3.1. Compute the moment tensors $\underline{\underline{\boldsymbol{\sigma}}}_j^{\mathrm{eq}}$ for the primal problem and $\underline{\underline{\tilde{\boldsymbol{\sigma}}}}_j^{\mathrm{eq}}$ for the dual problem from Definition 3.2.
- **ESTIMATE**. Compute the primal estimator η_j, the dual estimator $\tilde{\eta}_j$ and the nonconforming estimator $\eta_{j,\mathrm{NC}}$ proposed for the goal-oriented error estimation.
- **MARK**. Mark sets for each of the primal and dual problems:
  1. The Dörfler marking chooses a minimal subset $\mathcal{M}_j^{\mathrm{p}} \subset \mathcal{T}_j$ such that
  $$\theta\sum_{K\in\mathcal{T}_j}\eta_j^2(K) \le \sum_{K\in\mathcal{M}_j^{\mathrm{p}}}\eta_j^2(K).$$
  2. The Dörfler marking chooses a minimal subset $\mathcal{M}_j^{\mathrm{d}} \subset \mathcal{T}_j$ such that
  $$\theta\sum_{K\in\mathcal{T}_j}\tilde{\eta}_j^2(K) \le \sum_{K\in\mathcal{M}_j^{\mathrm{d}}}\tilde{\eta}_j^2(K).$$
  3. The Dörfler marking chooses a minimal subset $\mathcal{M}_j^{\mathrm{NC}} \subset \mathcal{T}_j$ such that
  $$\theta\sum_{K\in\mathcal{T}_j}\eta_{j,\mathrm{NC}}^2(K) \le \sum_{K\in\mathcal{M}_j^{\mathrm{NC}}}\eta_{j,\mathrm{NC}}^2(K).$$
  4. Set $\mathcal{M}_j := \mathcal{M}_j^{\mathrm{p}} \cup \mathcal{M}_j^{\mathrm{d}} \cup \mathcal{M}_j^{\mathrm{NC}}$ the union of marked sets found for primal, dual and nonconforming marking procedures above.
- **REFINE**. Compute the closure of $\mathcal{M}_j$ and generate a new triangulation $\mathcal{T}_{j+1}$ using newest vertex bisection method ([38]).
  Set $j := j+1$.

End While

6. Numerical experiments

In this section, some numerical results for the goal-oriented a posteriori estimations are presented for the C^0IPDG method of Section 5.1 with $k = 2$. The approximate goal functional is defined by

$$Q_h := Q(u_h) + \left(\underline{\underline{\boldsymbol{\sigma}}}_h^{\mathrm{eq}} - D^2 s_h, \tilde{\boldsymbol{\sigma}}_h^{\mathrm{m}}\right). \tag{6.1}$$

The primal and dual estimators are defined respectively by $\eta_h := \|D^2 s_h - \underline{\underline{\boldsymbol{\sigma}}}_h^{\mathrm{eq}}\|$ and $\tilde{\eta}_h := \|D^2\tilde{s}_h - \underline{\underline{\tilde{\boldsymbol{\sigma}}}}_h^{\mathrm{eq}}\|$. This gives the following error estimate from (4.16)

$$e_{h,\mathrm{goal}} := |Q(u) - Q_h| \le \frac{\eta_h\tilde{\eta}_h}{2} + |Q(s_h - u_h)| =: \eta_{h,\mathrm{goal}}^{\mathrm{abs}}, \tag{6.2}$$

where the higher-order data oscillation terms are not considered in the computations. The estimators are further localized for a mesh adaptation as

$$\eta_h^2 = \sum_{K\in\mathcal{T}_h}\eta_{h,K}^2 \text{ where } \eta_{h,K} := \|D^2 s_h - \underline{\underline{\boldsymbol{\sigma}}}_h^{\mathrm{eq}}\|_{L^2(K)},$$

$$\tilde{\eta}_h^2 = \sum_{K\in\mathcal{T}_h}\tilde{\eta}_{h,K}^2 \text{ where } \tilde{\eta}_{h,K} := \|D^2\tilde{s}_h - \underline{\underline{\tilde{\boldsymbol{\sigma}}}}_h^{\mathrm{eq}}\|_{L^2(K)} \text{ and}$$

$$\eta_{h,\mathrm{NC}}^2 = \sum_{K\in\mathcal{T}_h}\eta_{h,K,\mathrm{NC}}^2 \text{ where } \eta_{h,K,\mathrm{NC}} := |Q((s_h - u_h)\chi_K)|,$$

and χ_K is the characteristic function defined on $K \in \mathcal{T}_h$. We apply Algorithm 1 which follows standard adaptive procedure SOLVE, ESTIMATE, MARK and REFINE for the numerical examples below. For the experiments below, the penalty parameter σ for the C^0IPDG method is set to 20.

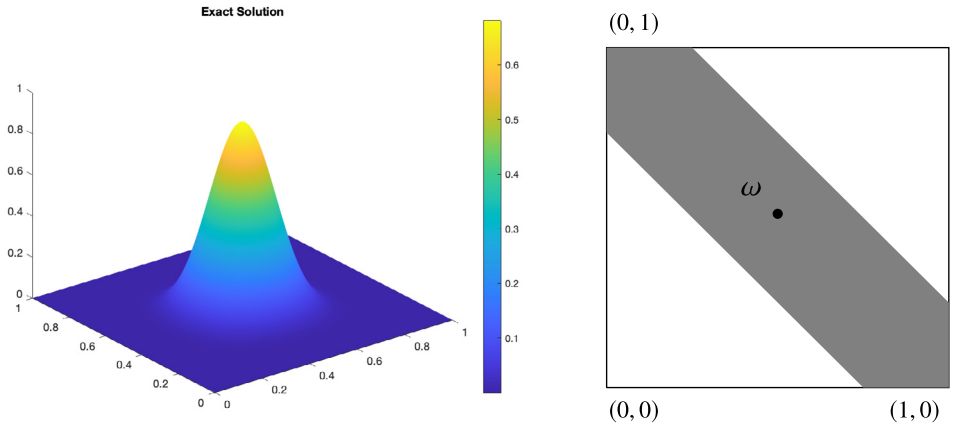

Fig. 1. The exact solution (*left*) and the zone of interest (*right*). Example 6.1, goal functional (6.4).

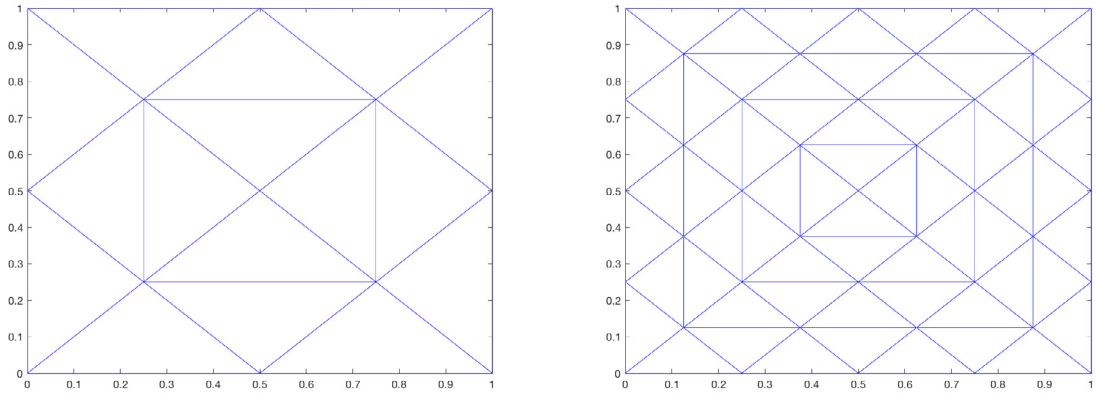

Fig. 2. (a) Initial triangulation $\mathcal{T}_0$ and (b) first uniform refinement $\mathcal{T}_1$ of Example 6.1.

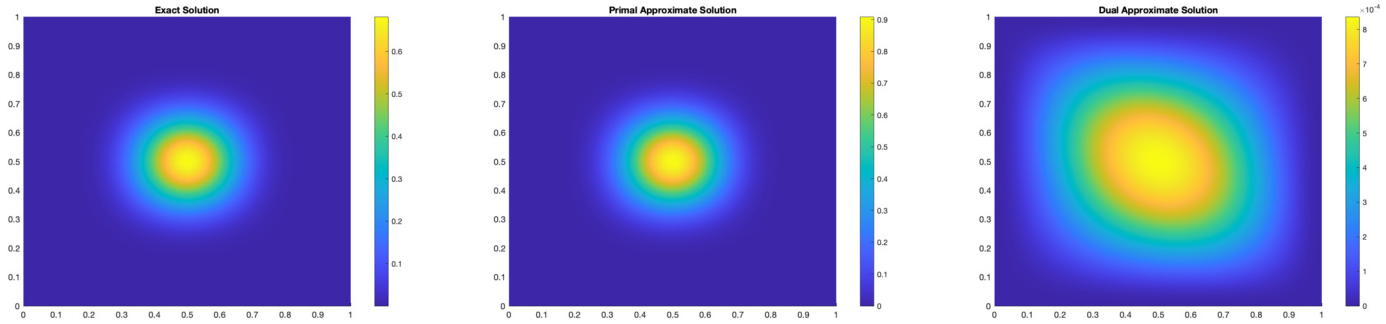

Fig. 3. The exact primal solution (*left*), the approximate primal solution (*middle*), and the approximate dual solution (*right*). Example 6.1, goal functional (6.4).

In the following numerical tests, we also compute the estimator found in (5.6) in the context of C^0IPDG method:

$$\eta^{\mathrm{res}}_{h,\mathrm{goal}} := \Big| \sum_{K\in\mathcal{T}_h} \int_K (\underline{\boldsymbol{\sigma}}^{\mathrm{eq}}_h - D^2 u_{\mathrm{IP}}) : \tilde{\underline{\boldsymbol{\sigma}}}^{\mathrm{eq}}_h \,\mathrm{dx} + \sum_{e\in\mathcal{E}_h} \int_e [\![\partial_n u_{\mathrm{IP}}]\!]_e \, \tilde{\sigma}^{\mathrm{eq}}_{h,nn} \,\mathrm{ds} \Big|, \quad (6.3)$$

where the absolute value has been taken in order to compare the estimator with the positive abstract goal estimator $\eta^{\mathrm{abs}}_{h,\mathrm{goal}}$. The potential reconstructions s_h and $\tilde{s}_h$ for the primal and dual solutions are computed from the definition in (5.4). The symmetric piecewise linear equilibrated moment tensors $\underline{\boldsymbol{\sigma}}^{\mathrm{eq}}_h$ for the primal and $\tilde{\underline{\boldsymbol{\sigma}}}^{\mathrm{eq}}_h$ for the dual problems are constructed from Lemma 5.1. The effectivity indices are computed by the ratio $\eta^{\mathrm{abs}}_{h,\mathrm{goal}}/e_{h,\mathrm{goal}}$ for abstract goal estimator $\eta^{\mathrm{abs}}_{h,\mathrm{goal}}$ and by $\eta^{\mathrm{res}}_{h,\mathrm{goal}}/e_{h,\mathrm{goal}}$ for the residual type goal estimator $\eta^{\mathrm{res}}_{h,\mathrm{goal}}$.

6.1. Regular solution and uniform refinements

In this test, we consider an exact solution defined on a plate $\Omega := (0,1)\times(0,1)$

$$u(x,y) = 10^{12} x^{10}(1-x)^{10} y^{10}(1-y)^{10}$$

with load function f defined by $f := \Delta^2 u$ in Ω. We consider a goal functional which is the mean value of the deflection around a strip $\omega \subset \Omega$, where the right-hand side function f, the solution u and gradient of u exhibit large changes. The exact solution has been illustrated in the left part of Fig. 1, and the zone of interest ω is highlighted by a grey colour in the right part of Fig. 1. The peak of the solution at $(\frac{1}{2}, \frac{1}{2})$ is highlighted by a bullet. The goal functional is defined by

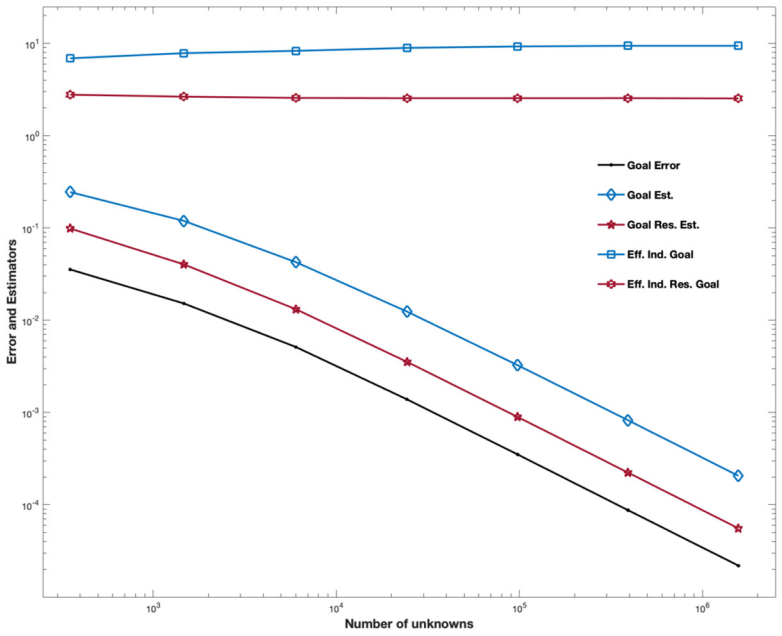

Fig. 4. The convergence histories for the goal error $e_{h,\mathrm{goal}}$, the abstract goal estimator $\eta^{\mathrm{abs}}_{h,\mathrm{goal}}$ and the residual estimator $\eta^{\mathrm{res}}_{h,\mathrm{goal}}$ with effectivity indices. Example 6.1, goal functional (6.4).

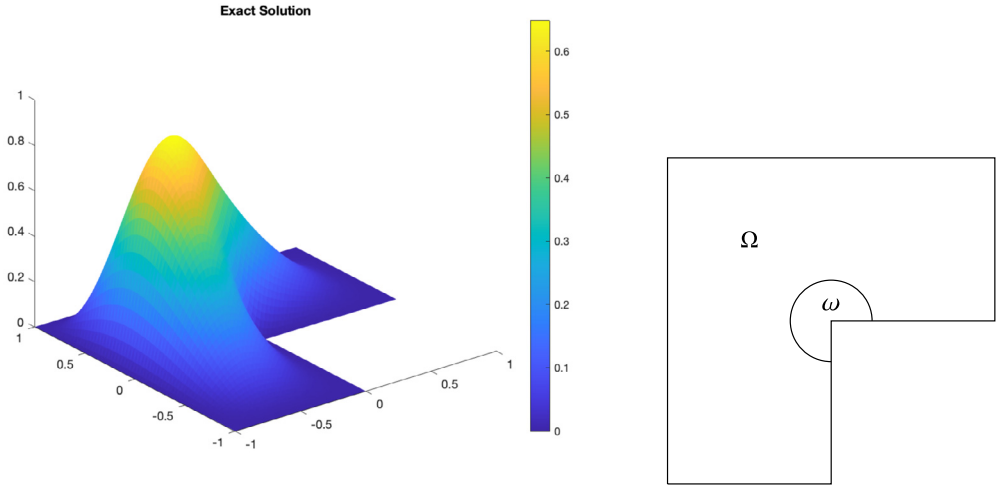

Fig. 5. The exact solution (*left*) and the zone of interest (*right*). Example 6.2, goal functional (6.5).

$$Q(u) = \frac{1}{|\omega|}\int_{\omega} u\,\mathrm{dx} = \left(\tilde{f}, u\right)_{\Omega}, \text{ with } \tilde{f} = \frac{\chi_{\omega}}{|\omega|}, \tag{6.4}$$

where the strip $\omega := \{(x,y) \in \Omega : 0.75 \le x + y \le 1.25\}$ is illustrated in the right side of Fig. 1 and χ_{ω} is the characteristic function defined on ω. The numerical integration value of the exact goal functional reads $Q(u) \approx 0.06044290015$.

Numerical experiments are performed on the sequence of uniform triangulations $\mathcal{T}_0, \mathcal{T}_1, \ldots, \mathcal{T}_5$ with the initial triangulation shown in Fig. 2(a). In the uniform refinement process, each triangle is subdivided into four similar triangles, see Fig. 2. In Fig. 3, the exact solution u in the left, the approximate primal solution u_{IP} in the middle, and the approximate dual solution $\tilde{u}_{\mathrm{IP}}$ in the right are projected on the domain Ω. The approximation for the goal function is found to be $Q_h = 0.06046477792$ on the mesh $\mathcal{T}_5$. The convergence histories for the goal error and goal estimator of (6.2) and (6.3) with respect to the number of unknowns are plotted in Fig. 4. We observe the quadratic convergence rates for the goal error and goal estimators with effectivity index close to 9.4 for the abstract goal estimator (6.2) and 2.5 for (6.3).

6.2. Singular solution and adaptive mesh refinement

In this test, we consider the L-shaped domain $\Omega = (-1,1)^2 \setminus \big([0,1) \times (-1,0]\big)$. Set the singular functions [23] $u(r,\theta) := (1 - r^2\cos^2\theta)^2(1 - r^2\sin^2\theta)^2 r^{1+\alpha} g_{\alpha,\omega}(\theta)$ with $g_{\alpha,\omega}(\theta) :=$

$$\begin{aligned}
&\Big(\frac{1}{\alpha-1}\sin\big((\alpha-1)\omega\big) - \frac{1}{\alpha+1}\sin\big((\alpha+1)\omega\big)\Big)\\
&\times\Big(\cos\big((\alpha-1)\theta\big) - \cos\big((\alpha+1)\theta\big)\Big)\\
&-\Big(\frac{1}{\alpha-1}\sin\big((\alpha-1)\theta\big) - \frac{1}{\alpha+1}\sin\big((\alpha+1)\theta\big)\Big)\\
&\times\Big(\cos\big((\alpha-1)\omega\big) - \cos\big((\alpha+1)\omega\big)\Big),
\end{aligned}$$

where the angle $\omega := \frac{3\pi}{2}$ and the parameter $\alpha = 0.5444837367$ is a non-characteristic root of $\sin^2(\alpha\omega) = \alpha^2\sin^2(\omega)$. It can be observed that the solution has the regularity $H^{2+\alpha}(\Omega) \cap H^2_0(\Omega)$, see [23]. Since the problem has a singularity at the origin $(0,0)$, we consider the goal functional

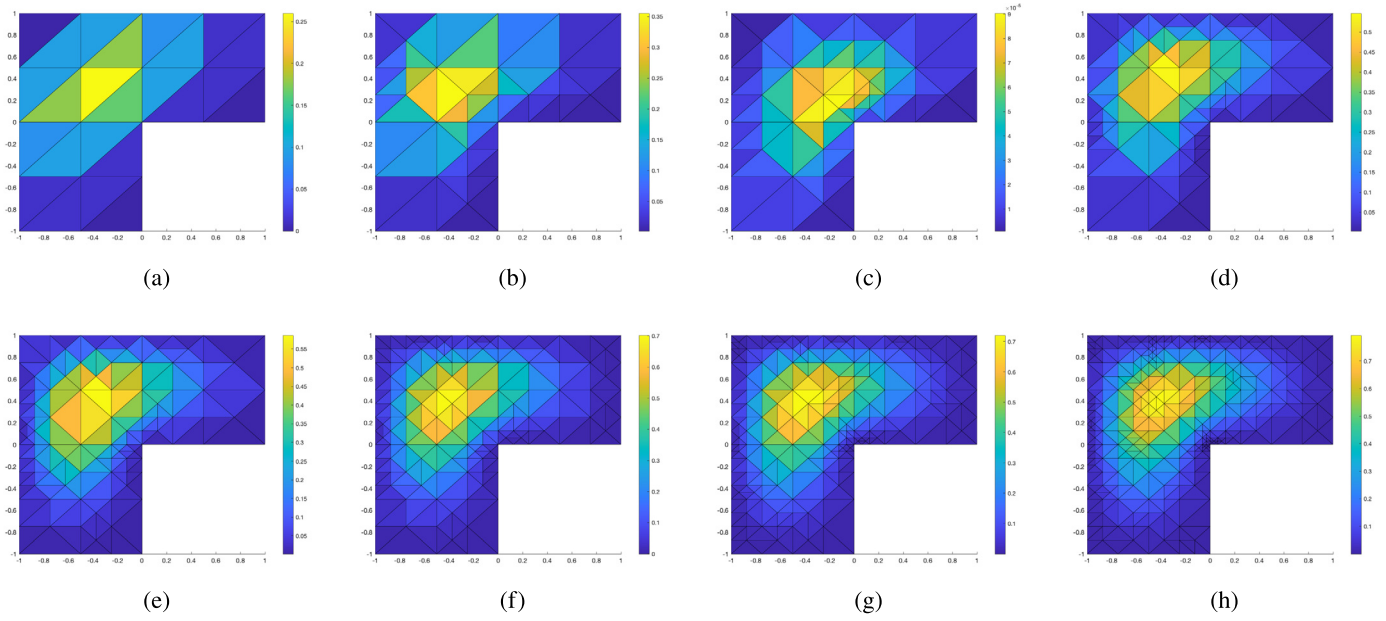

Fig. 6. The approximate primal solution u_{IP} on $\mathcal{T}_0, \mathcal{T}_1, \ldots \mathcal{T}_7$ with parameter $\theta = 0.25$ of Algorithm 1 for Example 6.2.

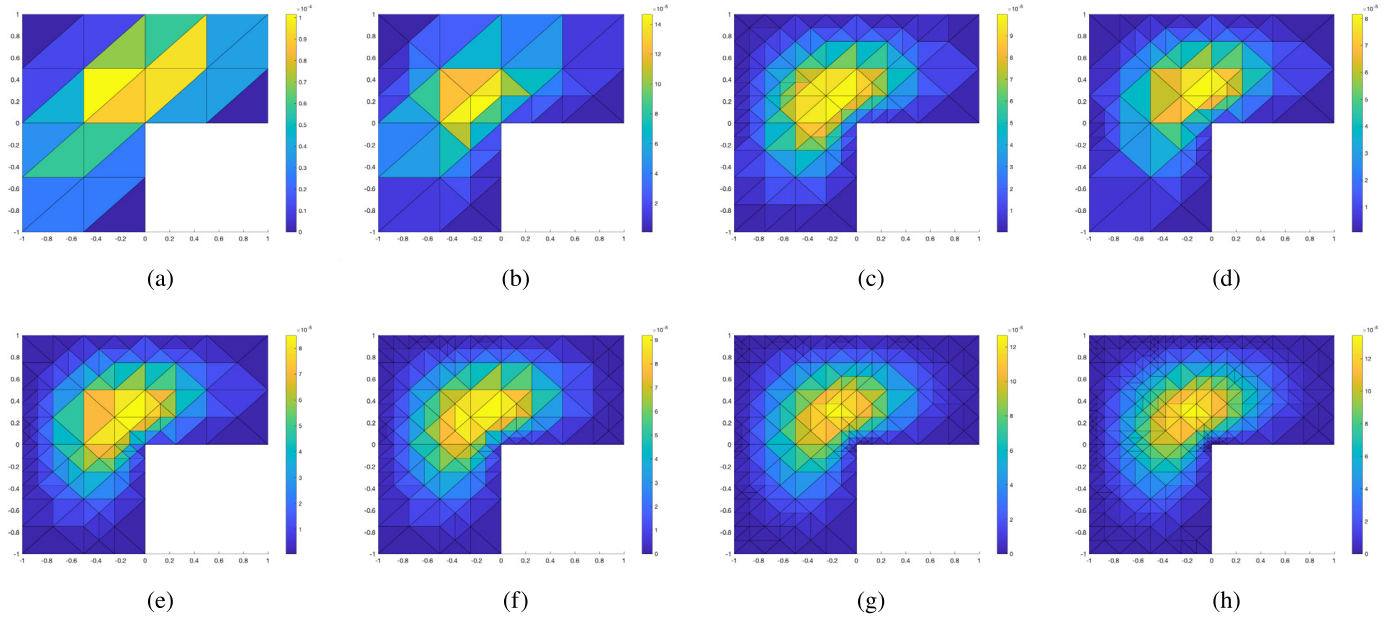

Fig. 7. The approximate dual solution $\tilde{u}_{\text{IP}}$ on $\mathcal{T}_0, \mathcal{T}_1, \ldots \mathcal{T}_7$ with parameter $\theta = 0.25$ of Algorithm 1 for Example 6.2.

$$Q(u) = \frac{1}{|\omega|}\int_{\omega} u\,\mathrm{dx} = \left(\tilde{f}, u\right)_{\Omega}, \text{ with } \tilde{f} = \frac{\chi_{\omega}}{|\omega|}, \tag{6.5}$$

where $\omega := \{(x, y) \in \Omega : (x-0)^2 + (y-0)^2 \leq 0.25^2\}$ and χ_{ω} is the characteristic function defined on ω. The exact solution (*left*), the domain Ω, and the zone of interest (*right*) are illustrated in Fig. 5. The numerical integration value of the exact goal functional reads $Q(u) \approx 0.018334438$.

For the numerical experiment, we start with an initial mesh $\mathcal{T}_0$ (see Fig. 8(a)). We apply the adaptive Algorithm 1 with refinement parameter $\theta = 0.25$ and maximum refinement level $J = 13$ to generate the adaptive meshes $\mathcal{T}_1, \mathcal{T}_2, \ldots, \mathcal{T}_{13}$. We also compare the results with the uniform refinement levels $\mathcal{T}_0, \mathcal{T}_1, \ldots, \mathcal{T}_5$. For the uniform refinement process, each triangle is divided into four similar triangles to obtain the next level mesh as described for the previous test. The initial mesh and final adaptive mesh are shown in Fig. 8. The adaptive meshes and projected solutions for the primal and the dual problems are illustrated in Figs. 6 & 7 for the first $\mathcal{T}_0, \mathcal{T}_1, \ldots, \mathcal{T}_7$ adaptive meshes. The convergence histories for the goal error and goal estimator of (6.2) and (6.3) with respect to the number of unknowns are plotted in Fig. 9 for the uniform and adaptive refinements. The goal error reduces for both the refinement procedures when the meshes are refined accordingly. Moreover, the convergence rate for adaptive refinements is higher than for uniform refinement. The adaptive algorithm helps to achieve higher accuracy for the approximation of goal functional with less number of unknowns in the computational process. The effectivity indices for the goal estimator $\eta^{\text{abs}}_{h,\text{goal}}$ and for the goal residual estimator $\eta_{h,\text{res}}$ on the uniform meshes appear to be close to 2 and 2.5, respectively. Whereas effectivity indices for these estimators for adaptive refinements appear to be close to 5 and 3, respectively.

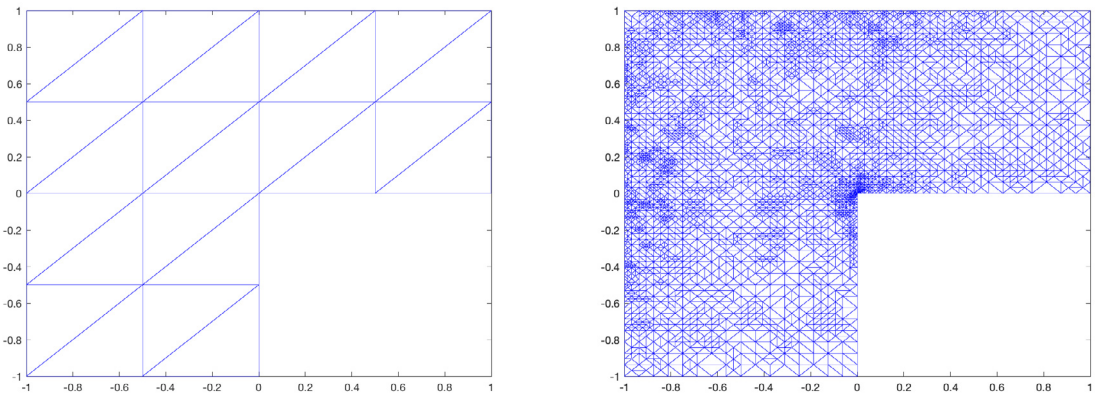

(a) (b)

Fig. 8. (a) Initial triangulation $\mathcal{T}_0$ and (b) adaptive mesh $\mathcal{T}_{13}$ with parameter $\theta = 0.25$ of Algorithm 1 for Example 6.2.

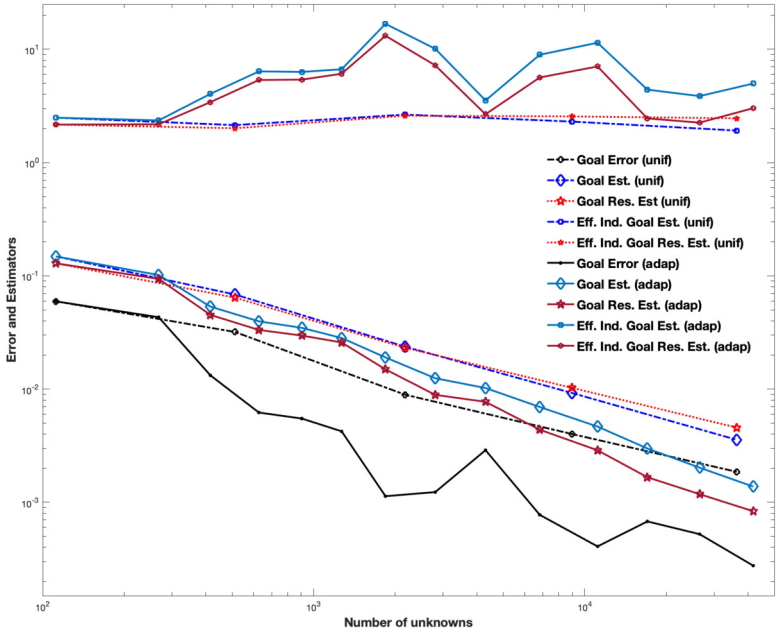

Fig. 9. The convergence histories for the goal error and the goal estimators with effectivity index for Example 6.2.

6.3. *Some shortcomings of the residual-based estimator of Theorem 4.1 and the abstract goal estimators of Theorem 4.3*

In this test, we consider the following problem setups. Let $\Omega := (-1,1)\times(-1,1)$. Consider the load function of the primal problem (3.1) as

$$f(x,y) = \begin{cases} 1 & \text{if } x>0 \text{ and } y>0, \\ -1 & \text{if } x<0 \text{ and } y<0, \\ 0 & \text{elsewhere,} \end{cases}$$

and the load function of the dual problem (3.4) is given by $\tilde{f} := \frac{1}{|\Omega|}$, i.e., the (global) mean deflection $Q(u) = \frac{1}{|\Omega|}\int_\Omega u\,\mathrm{dx}$. Due to the symmetry of the domain and the load function, the value of the mean deflection of the plate $Q(u) = 0$.

Numerical experiments are performed on the sequence of uniform meshes $\mathcal{T}_0, \mathcal{T}_1, \ldots, \mathcal{T}_3$ with the initial triangulation shown in Fig. 10(a). The computed solution u_{IP} for the primal problem using C^0IPDG method is illustrated in Fig. 10(b). The value of the computed goal functional on $\mathcal{T}_3$ is $Q(u_{\mathrm{IP}}) = -1.063258\times10^{-15}$, i.e., zero up to the machine precision. Therefore, the value of the simple goal error of (4.2) on $\mathcal{T}_3$ is

$$|Q(u) - Q(u_{\mathrm{IP}})| = 1.063258\times10^{-15} \ll \eta^{\mathrm{res}}_{h,\mathrm{goal}} = 4.501511\times10^{-5}. \tag{6.6}$$

This shows that for this kind of goal functional the residual estimator $\eta^{\mathrm{res}}_{h,\mathrm{goal}}$ highly over estimate the error with an effectivity index close to $+\infty$. The abstract goal estimator (4.16) provides the following error bound:

$$e_{h,\mathrm{goal}} = 1.763226\times10^{-6} \le \eta^{\mathrm{abs}}_{h,\mathrm{goal}} = 1.933562\times10^{-4}.$$

It provides a better structural error bound than the above residual-based estimator (6.6), but it still suffers from a high effectivity index close to 109.66.

7. Conclusion

This article presents an abstract framework of guaranteed goal-oriented a posteriori error control for the numerical approximation of a goal functional. We considered two popular discontinuous Galerkin finite element approximations for the biharmonic plate problem. The error in the approximation of the goal functional is represented by an estimator and by a remainder term that combines the dual-weighted residual method and the equilibrated moment tensor. The estimators

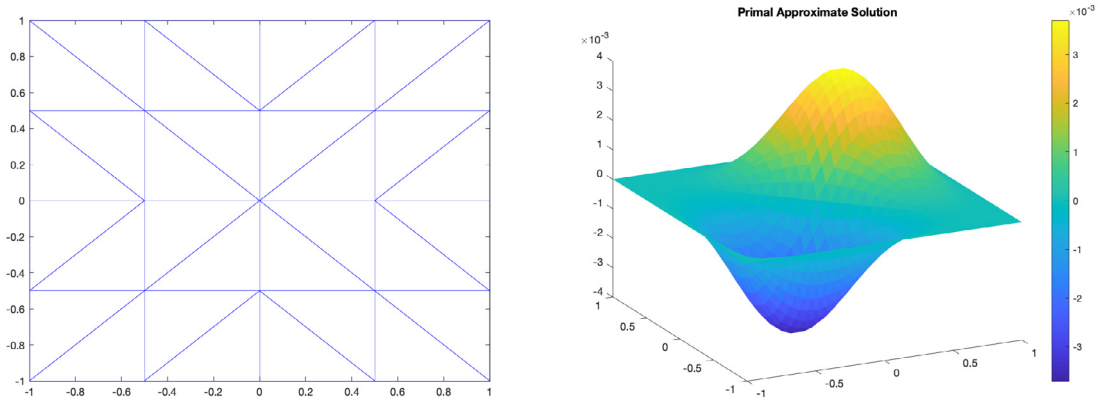

(a) (b)

Fig. 10. (a) Initial triangulation $\mathcal{T}_0$ and (b) the approximate primal solution u_{IP} on $\mathcal{T}_3$ for Example 6.3.

are based on the potential reconstruction and the equilibrated moment tensor that can be applied to various other finite element approximations. The methodology described in this article for the goal-oriented a posteriori error analysis can also be applied to nonlinear fourth-order plate problems.

Acknowledgements

The author would like to thank the DST C.V. Raman grant R(IA)/CVR-PDF/2020 and the National Board for Higher Mathematics (NBHM) research grant 0204/58/2018/R&D-II/14746 for the financial support.

References

[1] M. Ainsworth, R. Rankin, Guaranteed computable bounds on quantities of interest in finite element computations, Int. J. Numer. Methods Eng. 89 (2012) 1605–1634.
[2] W. Bangerth, R. Rannacher, Adaptive Finite Element Methods for Differential Equations, Lectures in Mathematics ETH Zürich, Birkhäuser Verlag, Basel, 2003.
[3] R. Becker, R. Rannacher, An optimal control approach to a posteriori error estimation in finite element methods, Acta Numer. 10 (2001) 1–102.
[4] D. Braess, Finite Elements, Theory, Fast Solvers, and Applications in Elasticity Theory, 3rd ed., Cambridge, 2007.
[5] D. Braess, R.H.W. Hoppe, C. Linsenmann, A two-energies principle for the biharmonic equation and an a posteriori error estimator for an interior penalty discontinuous Galerkin approximation, ESAIM: Math. Model. Numer. Anal. 52 (2018) 2479–2504.
[6] D. Braess, A.S. Pechstein, J. Schöberl, An equilibration-based a posteriori error bound for the biharmonic equation and two finite element methods, IMA J. Numer. Anal. 40 (2020) 951–975.
[7] S.C. Brenner, T. Gudi, L.-Y. Sung, An a posteriori error estimator for a quadratic C^0-interior penalty method for the biharmonic problem, IMA J. Numer. Anal. 30 (2010) 777–798.
[8] S.C. Brenner, L.R. Scott, The Mathematical Theory of Finite Element Methods, 3rd ed., Springer, 2007.
[9] S.C. Brenner, L.-Y. Sung, C^0 interior penalty methods for fourth order elliptic boundary value problems on polygonal domains, J. Sci. Comput. 22/23 (2005) 83–118.
[10] F. Brezzi, M. Fortin, Mixed and Hybrid Finite Element Methods, Springer Series in Computational Mathematics, vol. 15, Springer-Verlag, New York, 1991.
[11] M. Bürg, M. Nazarov, Goal-oriented adaptive finite element methods for elliptic problems revisited, J. Comput. Appl. Math. 287 (2015) 125–147.
[12] C. Carstensen, G. Mallik, N. Nataraj, A priori and a posteriori error control of discontinuous Galerkin finite element methods for the von Kármán equations, IMA J. Numer. Anal. 39 (2019) 167–200.
[13] J.H. Chaudhry, E.C. Cyr, K. Liu, T.A. Manteuffel, L.N. Olson, L. Tang, Enhancing least-squares finite element methods through a quantity-of-interest, SIAM J. Numer. Anal. 52 (2014) 3085–3105.
[14] P.G. Ciarlet, Interpolation error estimates for the reduced Hsieh-Clough-Tocher triangle, Math. Comput. 32 (1978) 335–344.
[15] M.I. Comodi, The Hellan-Herrmann-Johnson method: some new error estimates and postprocessing, Math. Comput. 52 (1989) 17–29.
[16] D.A. Di Pietro, A. Ern, Mathematical Aspects of Discontinuous Galerkin Methods, Mathématiques & Applications (Berlin) (Mathematics & Applications), vol. 69, Springer, Heidelberg, 2012.
[17] B. Endtmayer, T. Wick, A partition-of-unity dual-weighted residual approach for multi-objective goal functional error estimation applied to elliptic problems, Comput. Methods Appl. Math. 17 (2017) 575–599.
[18] T. Fraunholz, R.H.W. Hoppe, M. Peter, Convergence analysis of an adaptive interior penalty discontinuous Galerkin method for the biharmonic problem, J. Numer. Math. 23 (2015) 317–330.
[19] E.H. Georgoulis, P. Houston, Discontinuous Galerkin methods for the biharmonic problem, IMA J. Numer. Anal. 29 (2009) 573–594.
[20] E.H. Georgoulis, P. Houston, J. Virtanen, An a posteriori error indicator for discontinuous Galerkin approximations of fourth-order elliptic problems, IMA J. Numer. Anal. 31 (2011) 281–298.
[21] M.B. Giles, E. Süli, Adjoint methods for PDEs: a posteriori error analysis and post-processing by duality, Acta Numer. 11 (2002) 145–236.
[22] J.a.L. Gonçalves, S.M. Gomes, P.R.B. Devloo, A goal-oriented hp-adaptive discontinuous Galerkin approach for biharmonic problems, Int. J. Numer. Methods Eng. 97 (2014) 274–297.
[23] P. Grisvard, Singularities in Boundary Value Problems, vol. RMA 22, Masson & Springer-Verlag, 1992.
[24] T. Gudi, A new error analysis for discontinuous finite element methods for linear elliptic problems, Math. Comput. 79 (2010) 2169–2189.
[25] R. Hartmann, Multitarget error estimation and adaptivity in aerodynamic flow simulations, SIAM J. Sci. Comput. 31 (2008) 708–731.
[26] P. Ladevèze, Strict upper error bounds on computed outputs of interest in computational structural mechanics, Comput. Mech. 42 (2008) 271–286.
[27] P. Ladevèze, L. Chamoin, Calculation of strict error bounds for finite element approximations of non-linear pointwise quantities of interest, Int. J. Numer. Methods Eng. 84 (2010) 1638–1664.
[28] P. Ladevèze, F. Pled, L. Chamoin, New bounding techniques for goal-oriented error estimation applied to linear problems, Int. J. Numer. Methods Eng. 93 (2013) 1345–1380.
[29] G. Mallik, M. Vohralík, S. Yousef, Goal-oriented a posteriori error estimation for conforming and nonconforming approximations with inexact solvers, J. Comput. Appl. Math. 366 (2020) 112367.
[30] M.S. Mommer, R. Stevenson, A goal-oriented adaptive finite element method with convergence rates, SIAM J. Numer. Anal. 47 (2009) 861–886.
[31] I. Mozolevski, S. Prudhomme, Goal-oriented error estimation based on equilibrated-flux reconstruction for finite element approximations of elliptic problems, Comput. Methods Appl. Mech. Eng. 288 (2015) 127–145.
[32] J.T. Oden, S. Prudhomme, Goal-oriented error estimation and adaptivity for the finite element method, Comput. Math. Appl. 41 (2001) 735–756.
[33] W. Prager, J.L. Synge, Approximations in elasticity based on the concept of function space, Q. Appl. Math. 5 (1947) 241–269.
[34] S. Prudhomme, J.T. Oden, On goal-oriented error estimation for elliptic problems: application to the control of pointwise errors, in: New Advances in Computational Methods, Cachan, 1997, Comput. Methods Appl. Mech. Eng. 176 (1999) 313–331.
[35] V. Rey, P. Gosselet, C. Rey, Strict bounding of quantities of interest in computations based on domain decomposition, Comput. Methods Appl. Mech. Eng. 287 (2015) 212–228.
[36] V. Rey, P. Gosselet, C. Rey, Strict lower bounds with separation of sources of error in non-overlapping domain decomposition methods, Int. J. Numer. Methods Eng. 108 (2016) 1007–1029.

[37] V. Rey, C. Rey, P. Gosselet, A strict error bound with separated contributions of the discretization and of the iterative solver in non-overlapping domain decomposition methods, Comput. Methods Appl. Mech. Eng. 270 (2014) 293–303.
[38] R. Stevenson, The completion of locally refined simplicial partitions created by bisection, Math. Comput. 77 (2008) 227–241 (electronic).
[39] E.H. van Brummelen, S. Zhuk, G.J. van Zwieten, Worst-case multi-objective error estimation and adaptivity, Comput. Methods Appl. Mech. Eng. 313 (2017) 723–743.